Regular Article

Multistability, coexisting behaviours and control of fractional order dissipative small scale grid with disturbances and noise

Prakash Chandra Gupta[1,2,a] and Piyush Pratap Singh[1,2,b]

[1] Department of Electrical Engineering, NIT Meghalaya, Laitumkhrah, Shillong, Meghalaya 793003, India
[2] Electrical Engineering Department, National Institute of Technology Meghalaya, Laitumkhrah, Shillong, Meghalaya 793003, India

Abstract This paper introduces nonlinear analysis and control of a fraction order small-scale grid (SSG) under the influence of disturbances and noise. Random wind power supply and uncertain load demand are considered as disturbances while the additive white Gaussian noise is considered as external noise. The nonlinear dynamic behaviours such as multistability and coexisting bifurcation behaviours are investigated along with period-2, period doubling bifurcation route to chaos and instability (chaos breaking) of the rotor angle which is not expected under normal operating condition and reveal stability issue in the proposed SSG. Also, the presence of nontrivial behaviours, multistability and coexistence of attractors, may be of capital importance in understanding dynamic remedy of the fractional order SSG behaviour since serious impediments may occur even after the present required safeguard. An adaptive fractional second order PID sliding mode control (AFSO-PIDSMC) is proposed to control the chaos and multistability behaviours in the fractional order SSG. The proposed control technique includes the design adaptive control based on the designed fractional and second-order PID sliding mode control. Required asymptotic stability condition is derived by using Lyapunov stability theory. Furthermore, the proposed control technique is compared and has fast convergence, parameter estimation and chatter-free response. Numerical simulations are performed in MATLAB environment and validate the theoretical aspects.

1 Introduction

The dynamics of power systems are complex and nonlinear in nature, and the integration of renewable energy sources makes them even more complex. Despite the fact that complex and nonlinear analyses of large power system dynamics are extremely difficult, some small scale power systems such as the fundamental power system model [1, 2], single machine infinite bus power system model [3], and 4D power system model [4, 5] have been studied by utilizing the advanced nonlinear or chaos theories in the past. The research on small size power systems [6–8] (mini and micro grids etc.) have piqued the interest of scientific communities towards dynamic modeling and analysis of small scale power

system under the influence of uncertainties and disturbances [9–11]. The term "small-scale grid" refers to a power grid that connects producing plants and loads on a much more localised scale than is the case with traditional power grid. Small-scale grids are becoming increasingly popular in remote or rural areas where traditional power grids are not feasible. They often use renewable energy sources such as solar, wind, or hydropower. Furthermore, having a close connection between generators and loads helps to mitigate transmission loss and provides an energy efficient system. When compared to the use of purely traditional sources, the integration of RES into the grid results in increased efficiency and environmental friendliness. Small-scale grids can also provide greater energy security and independence, as they are less vulnerable to large-scale outages or disruptions that can occur in national grids, which is why an SSG is required [12]. Emergency rate-driven control of rotor angle instability is reported in a nonautonomous stochastic bi-stable power system oscillator [13]. Under the disruption of intermittent supply from renewable energy sources and other disturbances

Prakash Chandra Gupta and Piyush Pratap Singh have contributed equally to this work.

[a] e-mail: prakashgupta@nitm.ac.in (corresponding author)
[b] e-mail: piyushpratapsingh@gmail.com

like load fluctuations etc., the power system eventually exhibits chaotic oscillation and plays a vital role in the power system stability [14, 15]. Additionally, the influence of external disturbances such as random external parameter and noise excitation affect the chaotic oscillation and trigger the power system behaviour into multistability or even into chaos breaking behaviour [9, 16].

Chaos and multistability behaviours have been explored in the numerous nonlinear dynamical systems in the past [22–25] such as hyperjerk system based novel ANN-ring-based true random number generator [26], quasi-periodically forced system [27], Lu and Pan chaotic systems [28], multi synchronous machine model [29] etc. and analysed to that of fractional ordered counterpart as well and has received a lot of attention in recent years. Recently, fractional order calculus has been widely employed in many disciplines of science and engineering to study the dynamics, e.g. chaotic system [23], rub-impact rotor system [30], biological system [31], memristive system [32], Wien bridge oscillator [33], control and stabilisation [34–39], thermometric system [40], reaction-diffusion system [41], power system [42], control system [1, 43–48] etc.

Research on the fractional or non-integer order dynamic modeling is still under development and must go too far to be mature even though the researcher have

Table 1 Two-dimensional power system models with reported dynamic behaviours via analysed parameters

Studied 2-D power system model	Studied dynamic behaviour	Multistability behaviour	Analysis through parameter	Control technique
SMIB power system [10]	Chaotic motion and Melnikov analysis	No	Periodic load disturbance, damping coefficient	No
SMIB power systems [17]	Chaotic and non-chaotic regions using Melnikov analysis	No	Excitation frequency	No
Noisy SMIB power system [16]	Chaotic motion and basin erosion when the noise excitation is present	No	External noise intensity (Gaussian white noise)	No
Classical SMIB power systems [9]	Random parameter can induce and enhance chaos	No	Random perturbed parameter	No
Power system with wind power generator [18]	Chaotic state with certain value of random wind power	No	Amplitude of random wind power	Adaptive fuzzy control
SMIB power system [19]	Chaotic motion with Melnikov analysis	No	Two harmonic excitation disturbances (external periodic load and the outer mechanical disturbance)	No
Two-machine infinite-bus [20]	Bifurcation analysis without and with 1:3 internal resonance	No	Infinite-bus voltage amplitude and phase fluctuations	No
Fractional order Ship power system [21] (two-generator parallel-connected)	Chaotic response in fractional order range	Yes	System parameter values	No
Fractional order small scale grid (SSG) with disturbances and noise	PDB route to chaos, chaos breaking, multistability, coexisting behaviours	Yes and coexisting behaviour	Fractional order, electromagnetic power, random wind power, periodic load variation, amplitude of AWGN noise	Adaptive fractional second order PIDSMC

Eur. Phys. J. Spec. Top. (2023) 232:2415–2436

2417

intuition that the non-integer order dynamic models based on fractional calculus offer a more accurate representation of real-time systems [49]. Researchers have faith that the unlike traditional or integer order differentiation and integration, fractional calculus involves the differentiation or integration of non-integer orders and has tremendous potential in exploring a different way to see the model and control the nature around us [50]. Fractional order provides an extra degree of freedom, and fractional-order models may be able to better describe the dynamic behaviours of electromechanical systems and power systems. Fractional-order modeling in power systems offers improved accuracy, enhanced stability analysis, advanced control strategies, better representation of distributed energy resources, detailed frequency response analysis, and accurate modeling of power electronic devices [51–53]. These advantages make fractional order modeling a valuable tool for power system engineers and researchers in understanding, analyzing, and optimizing the operation of complex power systems.

In a dissipative dynamical system, multistability refers to the persistence of multiple alternative steady states with a given set of parameters. Multistability mainly depends upon initial conditions, as a result, the basin of attraction for multistable systems is complex [54]. Multistability has been observed in different fields such as chaotic systems [55, 56], electronic circuits [25], laser systems [57, 58], electromechanical systems [59–62], brain systems [63], neurons [64], including signal processing [65] etc. Multistability has feature of concern, due to the sudden shift to an undesirable attractor brings the worst or disastrous situation that has happened in the past, i.e. in 1992 YF-22 boeing crash [54], bridge collapse [66], and in other example such as failure of drilling rings with induction motor [59] that could have been prevented by controlling multistability.

Fractional order controller has significant advantages over integer order controller [47, 67–69] and widely been used in the literature [69–72]. In paper [47], a fractional order controller has been developed based on extremum seeking sliding mode control (SMC) technique and shows the significant advantages over integral controller. In paper [67], the fractional order SMC for velocity control of permanent magnet synchronous motor has been reported. A fractional order adaptive integral sliding surface based control law has been designed to control of robotic link manipulator [68]. Chatter free fractional order SMC has been reported in paper [70]. A fractional order proportional-integral-derivative (PID) SMC technique has been proposed [71] and significant advantages of $PI^\lambda D^\lambda$ sliding surface over PD^μ type sliding surface are highlighted. In paper [69], a $PI^\lambda D^\mu$ sliding surface based smooth fractional order SMC control has been studied to achieve fast and chatter free response.

In summary, the recent literature are focused on different fractional order sliding surfaces to have further improvement in the SMC design and application in fractional order nonlinear dynamical system but SMC control alone fails in estimating the unknown parameters,

disturbances and noise which play significant role and still requires an hybrid approach to counter such problem. Because in the disturbance or noise acting scenario, the linearisation of system dynamics is impossible and demands the analysis, control using the nonlinear theories/control. Further, the studied related power system models with explored behaviours and utilised control techniques are summarised in Table 1, where the bifurcation and chaos behaviours have been explored in all the integer order power system models but the coexisting and multistability behaviours and their control are not yet reported. The multistability behaviour is reported only in the fractional order ship power system [21]. Therefore, motivated with above problems and research gaps, the following objectives are considered:

1. To develop a fractional order SSG model where wind power generator and periodic load are integrated with synchronous generator.
2. To explore and control the unlike multistability or coexisting behaviours for redefining the counter measure in the fractional order SSG model.

In this paper, a novel fractional order small scale grid (SSG) model with disturbances, noise is proposed and examined the complex nonlinear phenomenon via varying fractional order, electromagnetic power and under the influence of random wind power, periodic load (disturbances), and additive white Gaussian noise (AWGN). Complex nonlinear phenomena such as different bifurcation behaviours, chaotic oscillation, coexisting attractors and multistability are analysed by using available qualitative and quantitative nonlinear tools. Further, an adaptive fractional second order PIDSMC (AFSO-PIDSMC) is designed and compared with recently reported robust adaptive fractional order sliding mode control (RAFOSMC) [73]. The proposed AFSO-PIDSMC technique has combined advantages of adaptive control and fractional second order sliding mode control techniques, and provides better accuracy, robust chatter free control, faster in response and unknown parameter estimation. The proposed AFSO-PIDSMC is also able to control multistability behaviour alongside chaos behaviour present in the fractional order SSG under the influence of disturbances and noise. The contribution and importance of this work are listed as follows:

1. A fractional order SSG with disturbances and noise is proposed and complex nonlinear phenomena are examined via varying fractional order, electromagnetic power and under the influence of random wind power, periodic load (disturbances) and additive white Gaussian noise (AWGN).
2. The fractional order SSG system exhibits regular and irregular behaviours like periodic-2, period doubling bifurcation (PDB) route to chaos and chaos breaking which leads to rotor angle instability.

2418

Eur. Phys. J. Spec. Top. (2023) 232:2415–2436

3. The fractional order SSG system has multistability and coexisting behaviours which may be of capital importance in the dynamic evolution of the SSG behaviour since serious impediment may occurs even after the present required safeguard.

4. The major benefit of the fractional SSG dynamics under study provides new insights in terms of coexisting behaviours or multistability compared to previous contributions [9–11, 13] and useful in redefining a new counter measure for dynamic remedies.

5. An AFSO-PIDSMC is designed to control the unwanted chaotic oscillations and compared with RAFOSMC [73] technique. The AFSO-PIDSMC has significant advantages such as fast convergence and chatter free response.

6. The proposed AFSO-PIDSMC technique is also capable of controlling multistability behaviour in fractional order SSG system.

We could not find such study in the literature and reflects the novelty of this work.

2 Fractional order small scale grid (SSG)

2.1 Preliminaries of fractional order calculus

Definition 1 [74]: The Riemann–Liouville definition of fractional differentiation and integration of qth-order function $f(t)$ is expressed as:

$$
\begin{cases}
{}_aD_t^q f(t) = \frac{1}{\Gamma(m-q)} \frac{\mathrm{d}^m}{\mathrm{d}t^m} \int_a^t \frac{f(\tau)}{(t-\tau)^{q-m+1}} \mathrm{d}\tau \\
{}_aD_t^{-q} f(t) = \frac{1}{\Gamma(q)} \int_a^t (t-\tau)^{q-1} f(\tau) \mathrm{d}\tau,
\end{cases}
\tag{1}
$$

where $(m-1) < q \leq m$, $m \in N$ and a is the initial time usually taken as 0, $\Gamma(.)$ represents the Gamma function.

Definition 2 [74]: The Caputo's definition of qth fractional order integration and differentiation of the function $f(t)$ is expressed as:

$$
{}_aD_t^q f(t) = \begin{cases}
\frac{1}{\Gamma(m-q)} \int_a^t \frac{f^m(\tau)}{(t-\tau)^{q-m+1}} \mathrm{d}\tau, & m-1 < q < m \\
\frac{\mathrm{d}^m}{\mathrm{d}t^m} f(t), & q = m
\end{cases}
\tag{2}
$$

where a is the initial time usually taken as 0 and m is the smallest integer such that $m \geq q$.

Properties [74]: The Riemann–Liouville's and Caputo's derivatives hold following conditions and denoted as "C^d" and "R^d", respectively.

1. $R^d \ {}_aD_t^q f(t) \left(R^d \ {}_aD_t^{-\beta} f(t) \right) = R^d \ {}_aD_t^{q-\beta} f(t)$, where $q \geq \beta \geq 0$.

2. $C^d \ {}_aD_t^q f(t) \left(C^d \ {}_aD_t^{-\beta} f(t) \right) = C^d \ {}_aD_t^{q-\beta} f(t)$, where $q \geq \beta \geq 0$.

3. The "R^d" fractional derivative has a composition rule such as $\frac{\mathrm{d}^m}{\mathrm{d}t^m} R^d \ {}_aD_t^q f(t) = R^d \ {}_aD_t^q \frac{\mathrm{d}^m}{\mathrm{d}t^m} f(t) = R^d \ {}_aD_t^{q+m} f(t)$, iff $f(t)$ satisfies the condition $f^s(a) = 0$ at $t = a$, where $s = 0, 1, 2, \ldots, m$, and $m = 0, 1, 2, \ldots, n-1 < q < n$.

4. The "C^d" fractional derivative has a composition rule such as $\frac{\mathrm{d}^m}{\mathrm{d}t^m} C^d \ {}_aD_t^q f(t) = C^d \ {}_aD_t^q \frac{\mathrm{d}^m}{\mathrm{d}t^m} f(t) = C^d \ {}_aD_t^{q+m} f(t)$, iff $f(t)$ satisfies the condition $f^s(a) = 0$ at $t = a$, where $s = n, n+1, n+2, \ldots, m$, for $m = 0, 1, 2, \ldots, n-1 < q < n$.

5. The "R^d" fractional derivative of constant is defined as $R^d \ {}_aD_t^q c = \frac{ct^{-q}}{\Gamma(1-q)}$, where c is a constant.

6. The "C^d" fractional derivative of constant is defined as $C^d \ {}_aD_t^q c = 0$, where c is a constant.

## 2.2 Mathematical modelling of fractional order SSG system

The model, shown in Fig. 1, is considered as small scale grid (SSG), where synchronous generator and wind turbine generator are delivering power through transmission lines with bus B1 and bus B2, respectively, T_1 and T_2 are equivalent transformers, L_1 is load, CB_1 and CB_2 are circuit breakers along the tie lines of SSG. A nonlinear system whose operating point and stability inevitably depend on nonlinearities, disturbances, external noise and induce major impact on the behaviour and performance is known as SSG. The motion equation [18] (also known as swing equation) describing the angle dynamics of the synchronous generator is written as follows:

$$
\frac{\mathrm{d}\omega}{\mathrm{d}t} = \frac{\mathrm{d}^2\delta}{\mathrm{d}t^2} = \frac{1}{H}[P_m - P_d - P_e]
\tag{3}
$$

where δ is the rotor angle, and ω is the angular velocity. The moment of inertia H of synchronous machine connected at bus $B1$. P_m and P_e are the mechanical and electromagnetic powers, respectively, P_d is the damping power.

In the SSG model shown in Fig. 1, the synchronous machine is considered as a non salient pole type and transmission line losses are assumed to be insignificant. Let the random wind power having amplitude P_w and frequency β_1, and periodic load disturbance (L_1) having amplitude P_d and frequency β_2 be integrated at bus B2. Then, the electromechnical swing equation by considering the random wind power [18] and periodic load disturbance [10] can be written as follows:

$$
\begin{cases}
\frac{\mathrm{d}\delta}{\mathrm{d}t} = \omega \\
\frac{\mathrm{d}\omega}{\mathrm{d}t} = \frac{1}{H}[P_m - P_s \sin\delta - D\omega + P_w \cos(\beta_1 t) + P_d \cos(\beta_2 t)].
\end{cases}
\tag{4}
$$
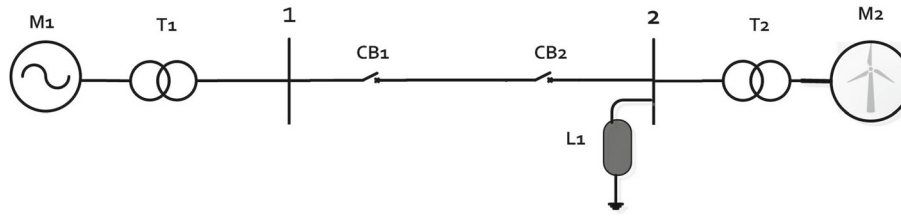
Fig. 1 Single line diagram of small-scale grid (SSG): M_1, denote synchronous generator and M_2, random wind power generator, T_1 and T_2 represents transformers, CB_1, CB_2, represent two circuit breakers, and L_1 represents local load

where D and P_s represents the damping coefficient and shaft power, respectively, of synchronous machine. Further, by assuming $\frac{P_m}{H} = \sigma$, $\frac{P_s}{H} = \rho$, $\frac{D}{H} = \lambda$, $\frac{P_w}{H} = \xi_w$, $\frac{P_d}{H} = \xi_p$, the system dynamics in (4) is simplified as

$$\begin{cases} \frac{d\delta}{dt} = \omega \\ \frac{d\omega}{dt} = \sigma - \rho \sin \delta - \lambda \omega + \xi_w \cos(\beta_1 t) + \xi_p \cos(\beta_2 t). \end{cases} \tag{5}$$

By introducing the Additive White Gaussian Noise [9] (AWGN) signal $\gamma(t)$, the noisy SSG dynamics can be written as

$$\begin{cases} \frac{d\delta}{dt} = \omega \\ \frac{d\omega}{dt} = \sigma - \rho \sin \delta - \lambda \omega + \xi_w \cos(\beta_1 t) + \xi_p \cos(\beta_2 t) + \xi_n \gamma(t). \end{cases} \tag{6}$$

where scaling factor ξ_n is the intensity of AWGN signal $\gamma(t)$.

Using the integral representation from the Caputo's fractional derivative *Definition* 2 [74], the SSG system dynamics (6) is written as

$$\begin{cases} {}_aD_t^q \delta = \frac{1}{\Gamma(1-q)} \int_a^t \frac{\omega(\tau)}{(t-\tau)^q} d\tau \\ {}_aD_t^q \omega = \frac{1}{\Gamma(1-q)} \int_a^t \frac{(\sigma - \rho \sin(\delta) - \lambda \omega + \xi_w \cos(\beta_1 \tau) + \xi_p \cos(\beta_2 \tau) + \xi_n \gamma(\tau))}{(t-\tau)^q} d\tau, \end{cases} \tag{7}$$

where $0 < q < 1$, and the derivatives are expressed as integrals involving the variable τ over the interval $[a, t]$. The Gamma function $\Gamma(1-q)$ is used in the denominator to ensure the proper scaling of the integral. Further, the fractional order dynamics of SSG system (7) is simplified as

$$\begin{cases} {}_aD_t^q \delta = \omega \\ {}_aD_t^q \omega = \sigma - \rho \sin \delta - \lambda \omega + \xi_w \cos(\beta_1 t) + \xi_p \cos(\beta_2 t) + \xi_n \gamma(t), \end{cases} \tag{8}$$

where ${}_aD_t^q$ denotes the Caputo's fractional derivative with order q.

Anomalous behaviours are analysed in the fractional order SSG system (8) and discussed in the next Section.

# 3 Dynamic analysis of fractional order SSG system

Here, the complex nonlinear behaviour are analysed and obtained by using nonlinear analysis tools such as bifurcation, Lyapunov exponents, time series and phase portrait analysis. The analysis of bifurcation behaviours of the fractional order SSG system is achieved in the steady state with observation time $T = 5000$ and step size $\Delta t = 0.01$, where the initial transient are discarded up to $T = 4000$ form the signal. Lyapunov exponents are also calculated using the Wolf algorithm [75] with the same observation time.

3.1 Dynamic behaviour vs fractional order derivative

The numerical simulation is performed using Caputo's fractional order calculus in MATLAB environment. The bifurcation behaviour is plotted with varying fractional order q of the SSG system (8). The bifurcation analysis is essential, particularly, for displaying different dynamic behaviours.

The order q of the differential equation is varied as $q \in [0.9, 1]$ and the value of other parameters are kept fixed as $\sigma = 0.2$, $\lambda = 0.02$, $\rho = 1.077$, $\xi_w = 0.2$, $\xi_p = 0.1$, $\xi_n = 0.01$ and with the initial condition $[\delta_0; \omega_0] = [1; -0.3]$, the bifurcation diagram is shown in Fig. 2a and phase plane behaviours at some specific values of q are shown in Fig. 2b–e. The obtained bifurcation diagram, shown in Fig. 2a, clearly shows that the SSG system (8) has period doubling bifurcation and chaos behaviours. These behaviours can also be verified via presented behaviours in the phase plane at different values of the fractional order as $q = 0.93$, $q = 0.96$, $q = 0.98$ and $q = 0.998$. The behaviours are period-2, period-4, at $q = 0.93$ and $q = 0.96$, respectively and chaos at $q = 0.98$, 0.998, shown in Fig. 2b–e. Lyapunov exponents are also calculated for the said two values of fractional order q where the SSG system (8) is showing chaos behaviour. For $q = 0.98$, the calculated Lyapunov exponents are $L_1 = 0.0179$ and $L_2 = -0.0399$. Similarly, for $q = 0.998$, the computed Lyapunov exponents are $L_1 = 0.0022$ and $L_2 = -0.0224$. At both the fractional order $q = 0.98$ and $q = 0.998$, the positive sign of the maximum Lyapunov exponent (MLE) confirms the presence of chaotic behaviour within the SSG system. Simultaneously, the sum of calculated Lyapunov exponents $L_1 + L_2$ at $q = 0.98$ and $q = 0.998$ are -0.022 and

2420

Eur. Phys. J. Spec. Top. (2023) 232:2415–2436
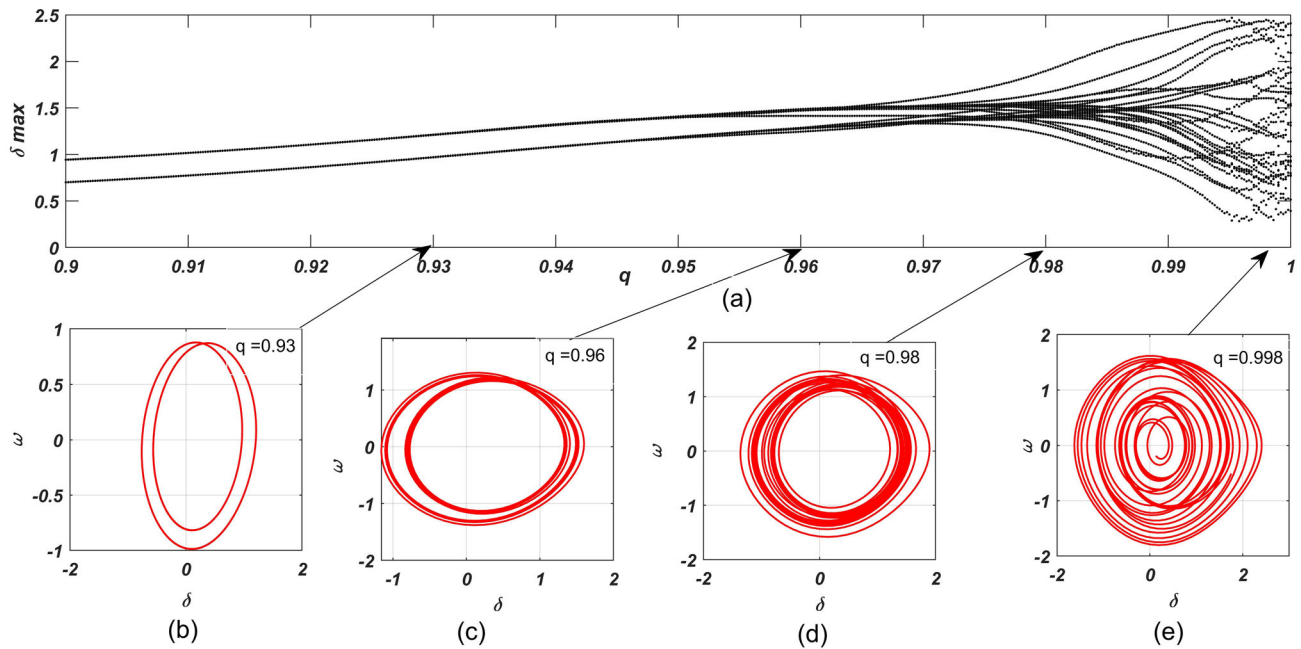
Fig. 2 a Bifurcation diagram of SSG system (8) when fractional order $q \in [0.9, 1]$ and the phase plane behaviours at specific value of fractional order in **b** $q = 0.93$, **c** $q = 0.96$, **d** $q = 0.98$, and **e** $q = 0.998$

−0.0202, respectively, conclude that the SSG system exhibits chaotic nature with a dissipative dynamics.

In this study, the order of fractional derivative is varied systematically and the system behaviours are observed through bifurcation and phase plane diagrams simultaneously, as illustrated in Fig. 2. Existing literature [76, 77] have revealed that the dynamic system does not exhibit chaos for lower orders of fractional derivative, and same is evident in our study where the chaos behaviour is obtained in the fractional order range $0.98 \leq q < 1$. The selection of $q = 0.98$ is motivated by selecting a smallest value of fractional order in the chaos range $q \in [0.98, 1)$ to study the chaotic and other significant phenomena in the SSG system, since the study at the fractional order say $q = 0.998 \approx 1$ does not provide significant difference to that of integer order counterpart.

3.2 Dynamic behaviour against the varying parameters of fractional order SSG system

In this section, different dynamic behaviours in fractional order SSG system (8) are explored with respect to four parameters such as the amplitude of electromagnetic power disturbances (ρ), random wind power variation (ξ_w), periodic load variation (ξ_p) and AWGN intensity (ξ_n). The fractional order is considered as $q = 0.98$ throughout. The Lyapunov exponents and corresponding dynamic behaviours at some particular values of bifurcation parameter in the specified ranges are listed in Table 2.

### 3.2.1 Dynamic behaviour by varing electromagnetic power

The amplitude of electromagnetic power ρ is chosen as a bifurcation parameter to explore the impact of electromagnetic power on a fractional order SSG system (8), while the other parameters are kept constant as $\sigma = 0.2$, $\lambda = 0.02$, $\xi_w = 0.2$, $\xi_p = 0.1$, $\xi_n = 0.01$.

Interestingly, as the amplitude of electromagnetic power ρ increases, the system begins with irregular behaviour such as chaos, then transitions to periodic motion and the unstable area via the backward and forward period-doubling bifurcation path depicted in Fig. 3. The range of varying electromagnetic power ρ is further subdivided into three ranges as $[0.9, 1.2] = [0.9, 0.976) \cup [0.976, 1.06] \cup (1.06, 1.2]$ to avoid difficulties in investigating or exploring the frequent changes in the obtained bifurcation behaviours shown in Fig. 3. Some specific parameter values are chosen in the three subdivided ranges and calculation of Lyapunov exponents and obtained dynamic behaviour are listed in Table 2. For example, in the range $\rho \in [0.9, 0.976)$, at $\rho = 0.927$ and $\rho = 0.96$, the nature of maximum positive Lyapunov exponent (MLE) is found (+ve) and indicates chaos behaviour, and at $\rho = 0.973$, the nature of MLE is (≈ 0) which indicates unstable behaviour (blank space in the bifurcation diagram). The blank space in the bifurcation diagram suggests that δ_{max} peak does not exist in the steady state, implying that the generator rotor angle (δ) has unstable behaviour. In order to have graphical validation, the time series and phase portrait behaviours of SSG system under chaos behaviour at $\rho = 0.96$ and unstable or chaos breaking behaviour at $\rho = 0.973$ are shown in Figs. 4 and 5, respectively.

Table 2 Lyapunov exponents and dynamic behaviour at specific value of bifurcation parameter in the defined range for SSG (8) (in reference to bifurcation diagram shown in Figs. 3, 6, 7 and 8)

Bifurcation parameter	Parameter range	Specific parameter value	Lyapunov Exponents L_1 & L_2	Dynamic behaviour
ρ	$\in [0.9, 0.976)$	$\rho = 0.927$ $\rho = 0.96$ $\rho = 0.973$	$(0.02934, -0.04957)$ $(0.09371, -0.01826)$ $(0.00056, -0.01947)$	Irregular (chaos, unstable)
	$\in [0.976, 1.06]$	$\rho = 1.0$ $\rho = 1.02$	$(-0.00973, -0.01081)$ $(-0.00956, -0.01832)$	Regular (periodic)
	$\in (1.06, 1.2]$	$\rho = 1.07$ $\rho = 1.09$ $\rho = 1.1$	$(0.02431, -0.03927)$ $(0.02401, -0.04635)$ $(0.000536, -0.00234)$	Irregular (chaos, unstable)
ξ_w	$\in [0, 0.2]$	$\xi_w = 0.1$ $\xi_w = 0.15$	$(-0.00986, -0.01043)$ $(-0.00986, -0.01321)$	Regular (Periodic)
	$\in (0.2, 0.25]$	$\xi_w = 0.2058$ $\xi_w = 0.225$ $\xi_w = 0.23$	$(0.00337, -0.02338)$ $(0.000292, -0.00431)$ $(0.00329, -0.02436)$	Irregular (chaos, unstable)
ξ_p	$\in [0.08, 0.116]$	$\xi_p = 0.095$ $\xi_p = 0.1$	$(-0.00923, -0.02350)$ $(-0.0109, -0.01089)$	Regular (periodic)
	$\in (0.116, 0.12]$	$\xi_p = 0.110$ $\xi_p = 0.12$	$(0.00362, -0.02349)$ $(0.00869, -0.01156)$	Irregular (chaos, unstable)
ξ_n	$\in [0.002, 0.014]$	$\xi_n = 0.006$ $\xi_n = 0.008$	$(-0.00952, -0.01024)$ $(-0.00963, -0.01243)$	Regular (periodic)
	$\in (0.014, 0.016]$	$\xi_n = 0.015$ $\xi_n = 0.016$	$(0.00232, -0.02342)$ $(0.00212, -0.02234)$	Irregular (chaos, unstable)

Fig. 3 Bifurcation behaviour of fractional order SSG system (8) with respect to varying electromagnetic power (ρ)

2422

Eur. Phys. J. Spec. Top. (2023) 232:2415–2436
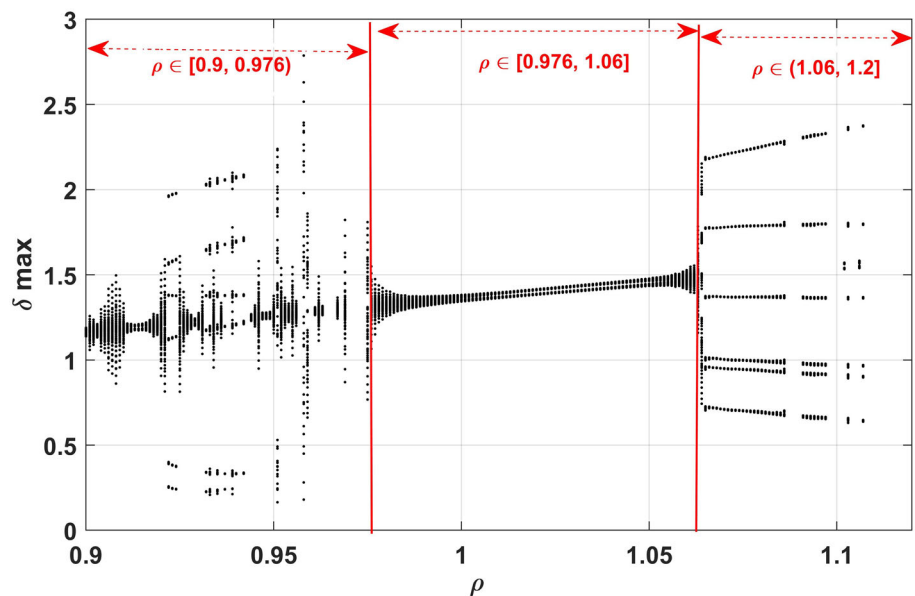
Fig. 4 Time series and phase plane diagrams of fractional order SSG system (8) at $\rho = 0.96$ reflect chaos behaviour
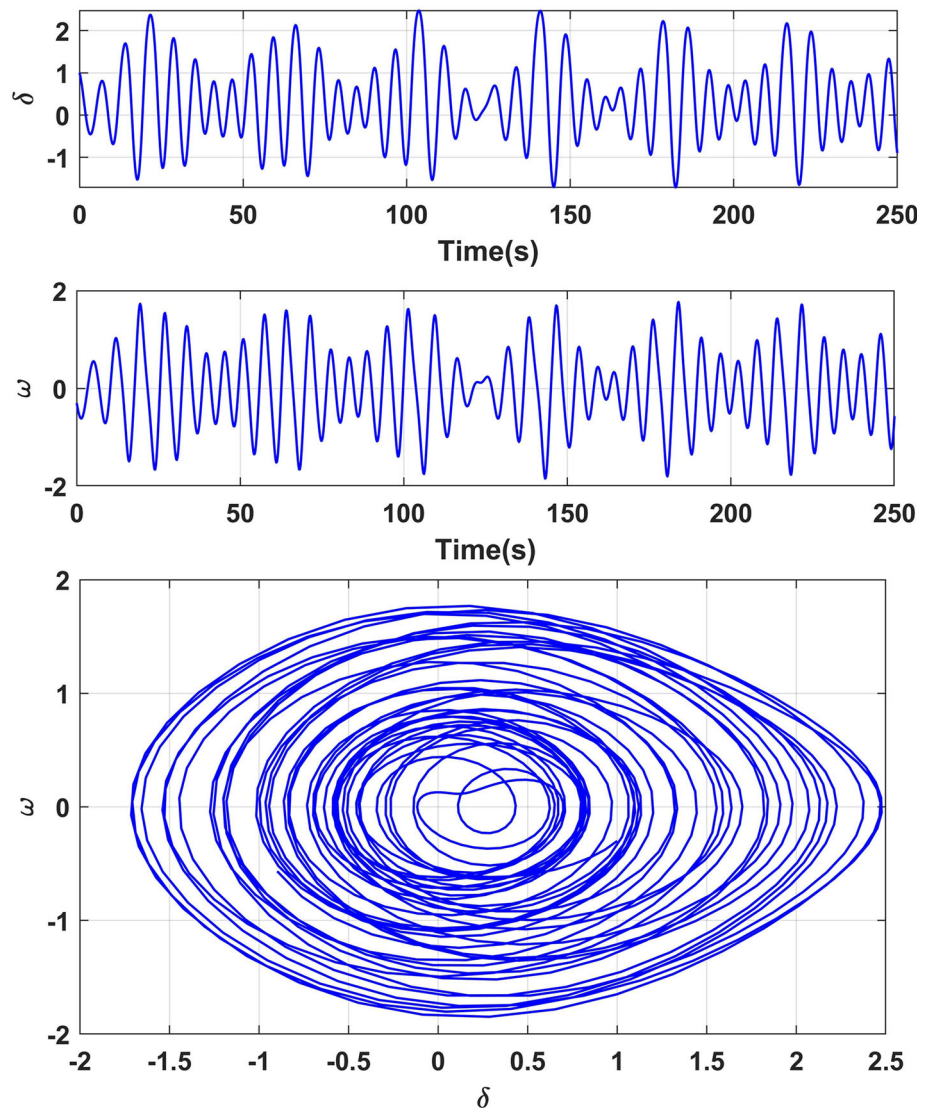
In the ranges $\rho \in [0.9, 0.976)$ and $\rho \in (1.06, 1.2]$, the bifurcation behaviour has frequent transitions between chaos to unstable and unstable to chaos, and referred as *irregular behaviour*. Similarly, in the range $\rho \in [0.976, 1.06]$, the $(-$ve$)$ MLE indicates periodic or PDB behaviours, and termed as regular behaviour. It is clear from the preceding discussion that electromagnetic power ρ disturbance can force the fractional order SSG system into chaotic oscillation or even unstable (breaking of chaos), can result in angle instability which is undesirable for stable operation of the SSG system or other power grids as well.

3.2.2 Dynamic behaviour by varing random wind power

To study the impact of random wind power on the fractional order SSG system, amplitude of the random wind power (ξ_w) is varied as a bifurcation parameter and the other parameters are kept fixed as $\sigma = 0.2$, $\lambda = 0.02$, $\rho = 1.077$, $\xi_p = 0.1$, $\xi_n = 0.01$. Bifurcation

diagram is obtained to analyse the effect of varying random wind power (ξ_w) parameter in the range $\xi_w \in [0, 0.25]$ and shown in Fig. 6. The obtained bifurcation diagram in the entire range $\xi_w = [0, 0.25]$ is divided into two ranges as $[0, 0.2] \cup (0.2, 0.25]$ and accordingly regular (periodic) and irregular (chaos, unstable) dynamic behaviours are obtained. Two specific values are chosen as $\xi_w = 0.1$ and $\xi_w = 0.15$ from the range $\xi_w \in [0, 0.2]$ for clear understanding and Lyapunov exponents are calculated. The nature of MLE at both the specified ξ_w values is $(-$ve$)$, indicating that the behaviour is regular (periodic) as listed in Table 2. In the range of $\xi_w \in (0.2, 0.25]$, the nature of MLE at $\xi_w = 0.2058$ and $\xi_w = 0.23$ is $(+$ve$)$ which indicates the irregular (chaotic) behaviour and at $\xi_w = 0.225$, the MLE is ≈ 0 confirms irregular (unstable) behaviour. Therefore, the fractional order SSG system exhibits irregular behaviour once the strength of random wind power increases as $\xi_w \geq 0.225$.

It is clear from the this study that random wind power ξ_w, acting as a disturbance, and can shift the

Fig. 5 Time series and phase plane plots of fractional order SSG system (8) at $\rho = 0.973$ show unstable (chaos breaking) behaviour
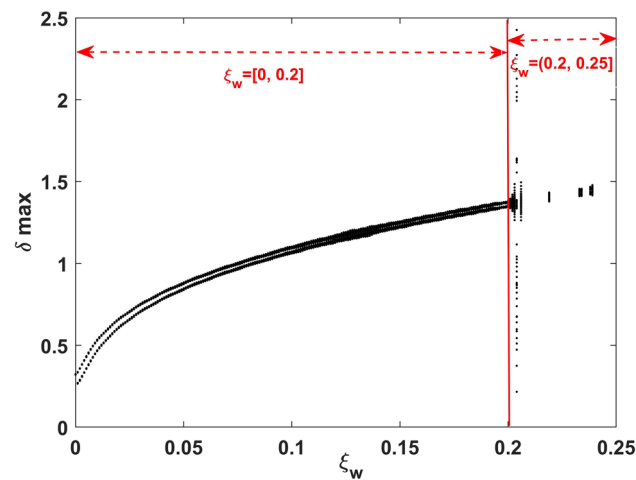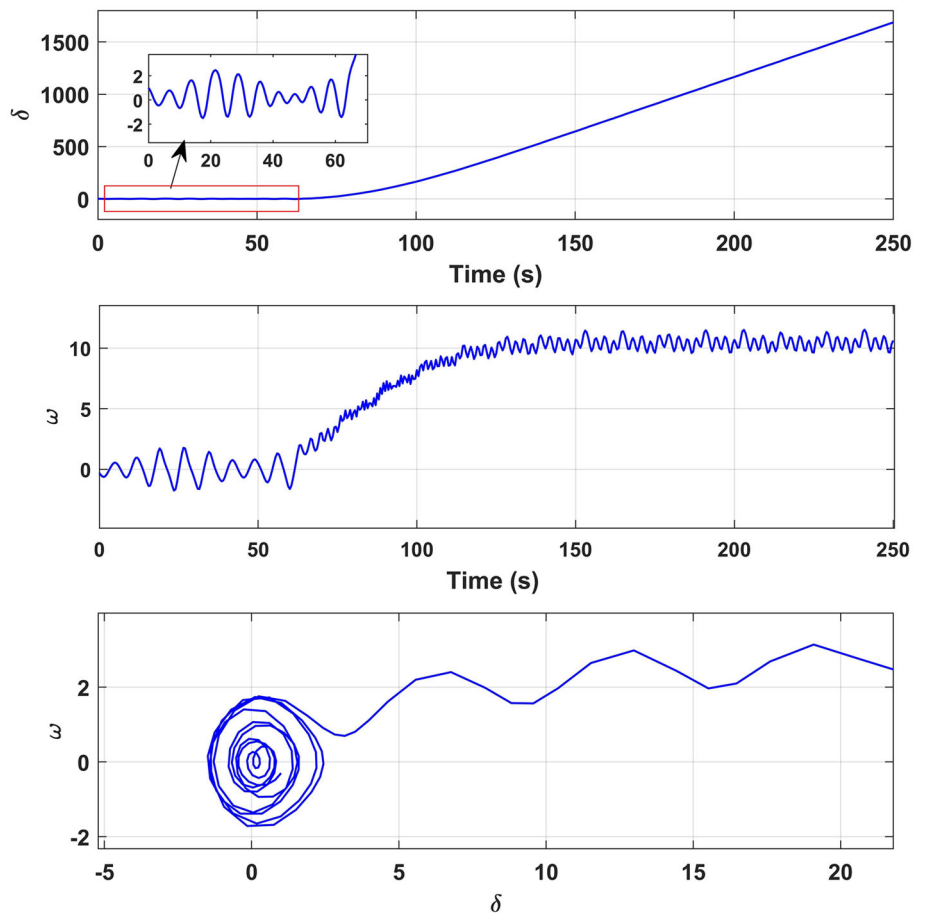
Fig. 6 Bifurcation diagram of fractional order SSG system (8) under the varying amplitude of random wind power (ξ_w)

periodic operating region into an irregular region such as chaotic or unstable. It also exclaims about the acceptable operating range of wind power and may be useful in tuning parameters in specified range. Therefore, it is important to study the effect of random wind power on the stability of the system and determine the acceptable range of wind power for safe operation.

This information can be used to optimise the system's parameters within a safe and stable operating range.

3.2.3 Dynamic behaviour with change in periodic load variation

In this subsection, the amplitude of periodic load (ξ_p) is considered as a bifurcation parameter and the remaining SSG parameters are kept fixed as $\sigma = 0.2$, $\lambda = 0.02$, $\rho = 1.077$, $\xi_w = 0.2$, $\xi_n = 0.01$. Bifurcation diagrams with respect to varying (ξ_p) parameter in the range $\xi_p \in [0.08, 0.12]$ is shown in Fig. 7 and it is apparent that fractional order SSG system has PDB route to chaos.

Furthermore, it is evident that the behaviour is periodic in the range $\xi_p \in [0.08, 0.116]$ and irregular in the range $\xi_p \in (0.116, 0.12]$. At some particular values of ξ_p in the specified ranges, the calculated Lyapunov exponents are listed in the Table 2. Therefore, it may be concluded that the periodic load variation may also force the SSG system into irregular (chaos, unstable) behaviour.

3.2.4 Dynamic behaviour by changing external noise

The intensity of AWGN (ξ_n) is selected as a bifurcation parameter to study the impact of AWGN on fractional

2424

Eur. Phys. J. Spec. Top. (2023) 232:2415–2436
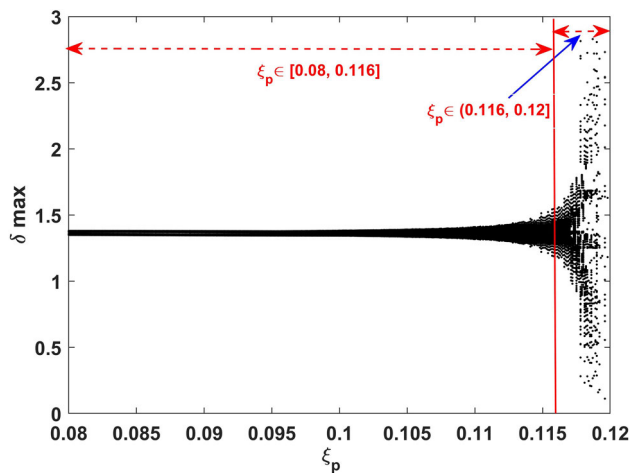
Fig. 7 Bifurcation behaviour of fractional order SSG system (8) under the varying amplitude (ξ_p) of periodic load variation
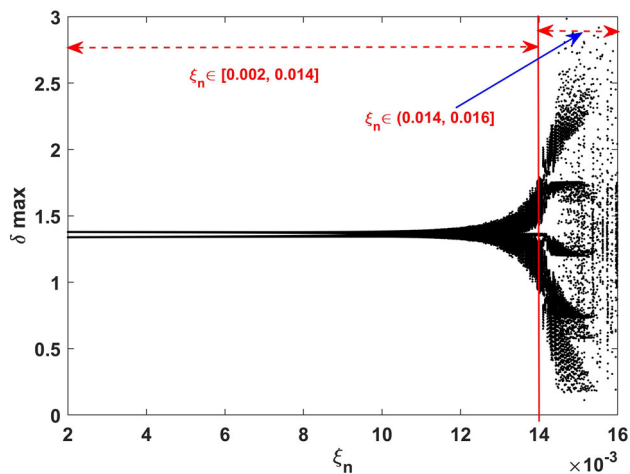
Fig. 8 Bifurcation diagram shows dynamic evolution of fractional order SSG system (8) under the varied range of AWGN intensity (ξ_n)

order SSG system where the other remaining parameters are fixed as $\sigma = 0.2$, $\lambda = 0.02$, $\rho = 1.077$, $\xi_w = 0.2$, $\xi_p = 0.1$. Bifurcation diagram are plotted in the varied range of parameter as $\xi_n \in [0.002, 0.016]$.

It is apparent from the bifurcation diagram (refer Fig. 8) that $\delta_{\max}$ of the fractional order SSG system has period-2 behaviour in the range $\xi_n \in [0.002, 0.014]$. At two values of $\delta_{\max}$ in the said range, the calculated Lyapunov exponents are listed in Table 2 which verify the obtained regular (periodic) behaviour since the nature of MLE is $-$ve. In the remaining range $\xi_n \in (0.014, 0.016]$, it is evident that the behaviour is frequently switching to either chaotic or unstable. Thus, the behaviour in the entire range is claimed as irregular and Table 2 may be referred for calculated Lyapunov exponent or nature of MLE and corresponding dynamic behaviour.

It may be remarked that by changing the SSG system parameters, different regular and irregular behaviours, including periodic and chaos, are observed in the fractional order SSG system. Further, if the chaos breaks, it can cause divergence in the machine angle, which leads to angular instability in the fractional order SSG system. This study is useful for selecting the appropriate range of parameters to design an effective controller as a result of the preceding discussions in this section.

## 4 Multistability and coexisting behaviours of fractional order SSG system

In this section, advent of interesting behaviours like multistability and coexisting behaviours of the fractional order SSG system are presented and discussed under the varying initial excitation of rotor angle δ_0 and the fractional order q. When all system parameter are considered as, $\rho = 1.07$, $\sigma = 0.2$, $\lambda = 0.02$, $\xi_w = 0.2$, $\xi_p = 0.1$, $\xi_n = 0.01$ are maintained constant. The initial condition $\omega_0 = -0.3$ is fixed and δ_0 is varied such that $\delta_0 \in (-15, 15)$ and plotted the bifurcation diagram as shown in Fig. 9. In the varied range of δ_0, repetition of similar bifurcation pattern is observed at regular interval and confirm the presence of multistability behaviour in the fractional order SSG system (8). It is also evident that each bifurcation pattern (refer the zoomed view in Fig. 9) has periodic-6, chaos, unstable behaviours.

Further, the phase portraits (δ vs ω) corresponding to bifurcation diagrams for varied range of δ_0 and fractional order q are plotted at some particular values of initial condition [δ_0; ω_0] and fractional order q and are shown in Fig. 10. Observing the phase portrait behaviours obtained at four different values of fractional order as $q = 0.93$, 0.96, 0.98 and 0.998, from top to bottom in Fig. 10, show multistability of PDB route to chaos behaviour in the fractional order SSG system. The five different values of initial conditions [δ_0; ω_0] are considered as [1; -0.3], [± 6; -0.3], [± 12.5; -0.3] for first to fifth columns.

The coexisting bifurcation behaviour is also found under varying fraction order as $q \in [0.9, 1]$ and initial conditions. The bifurcation plots are obtained by collecting the peaks of synchronous generator rotor angle δ at three initial conditions labeled as black colour when $(\delta_0, \omega_0) = (1, -0.3)$, red colour when $(\delta_0, \omega_0) = (0.8, -0.3)$, and blue colour when $(\delta_0, \omega_0) = (-1.8, -0.3)$ and shown in Fig. 11 which clearly shows the coexistence of similar and different bifurcation behaviours. At $q = 0.98$, the coexistence of periodic (regular) and chaotic (irregular) attractors is achieved (bottom left phase portrait in Fig. 11) and as the fractional order is increased to $q = 0.998$, chaotic and unstable attractors coexist, i.e. coexistence of irregular behaviours is evident and shown in Fig. 11, the bottom right phase portrait. The presence of coexisting or multistability behaviour in the fractional order SSG system leads to a shift in its operating point without any change in
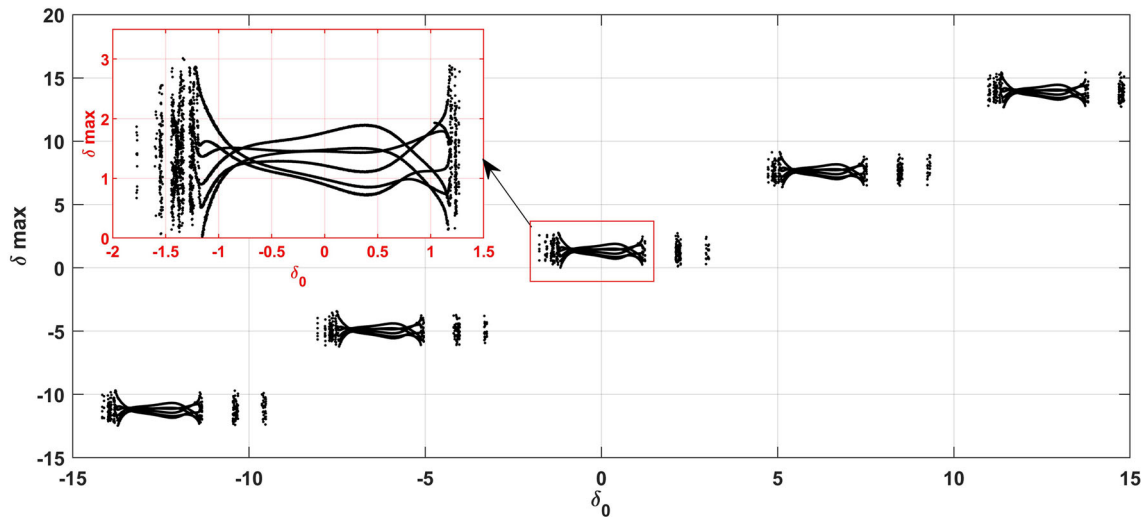
Fig. 9 Bifurcation behaviour of the fractional order SSG system (8) at initial condition $[\delta_0; \ \omega_0 = -0.3]$, where synchronous generator varies as $\delta_0 \in (-15, 15)$
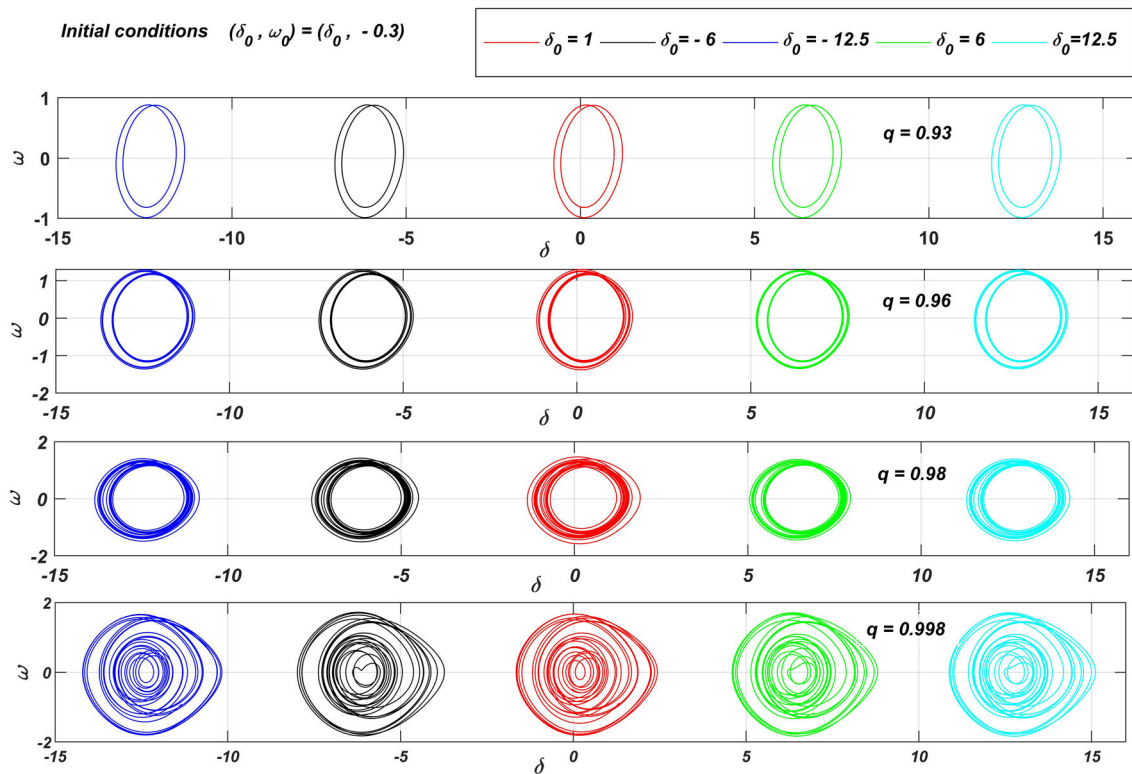
Fig. 10 Multistability of PDB to chaos behaviours shown via phase portrait plots at five different values of initial conditions $[\delta_0; \ \omega_0]$ as $[1; \ -0.3]$, $[\pm 6; \ -0.3]$, $[\pm 12.5; \ -0.3]$ and four values of fractional order (q) simultaneously

parameters. This shift indicates that the SSG has the potential either to get trapped into normal equilibrium, or risk to fall under sustained/chaotic oscillation.

Remark 1 In a power system, protective devices such as current and voltage transformers, relays, circuit breakers, the major required safeguards are designed to respond and mitigate transient conditions, such as short circuits or sudden voltage fluctuations. Typically, these devices are not intended to interfere with sustained oscillatory events like chaotic oscillation [78]. Consequently, chaotic operation for an extended period or even several minutes may damage expensive equipment like rotor shafts. Simultaneously, the wide frequency range of chaotic oscillations can introduce harmful harmonic transients in synchronous machines, further complicating the regular operation of the power system. It

2426

Eur. Phys. J. Spec. Top. (2023) 232:2415–2436

suggests that even with current safeguards, challenges or difficulties can arise in managing or controlling the system's behaviour due to the complex dynamics associated with chaos and multistability.

5 Adaptive fractional second order-PID sliding mode control (AFSO-PIDSMC)

In this section, design of adaptive fractional second order sliding mode control via proportional integral derivative sliding surface (PIDSMC) is discussed. The generalised block diagram of proposed control is shown in Fig. 12. The generalised fractional order $q \in (0, 1)$, n-dimensional nonlinear dynamical system under disturbances and noise can be written as:

$$D^q X = f(X, t) + G(t) + D^r(t) + u_i, \qquad (9)$$

where X, $f(X, t) \in \mathbb{R}^n$ are state variables and known nonlinear terms, respectively. $G(t)$, $D^r(t)$ are the unknown nonlinear terms as $G(t) \in \mathbb{R}^n$ and $D^r(t) \in \mathbb{R}^n$ represent disturbances and external noise, respectively, in the n-dimensional system. $u_i = [u_1, u_2, \ldots, u_n]^T \in \mathbb{R}^n$ is the added control input. Assuming that the disturbances and noise have varying amplitude such as $G(t) = \gamma_1 G_1(t) + \gamma_2 G_2(t)$, and $D^r(t) = \gamma_3 D^r(t)$, respectively, where γ_1, γ_2 are the varying amplitudes of two disturbances and γ_3 is the varying amplitude of external noise. Then Eq. (9) can further be written as:

$$D^q X = f(X, t) + \gamma_1 G_1(t) + \gamma_2 G_2(t) + \gamma_3 D^r(t) + u_i. \qquad (10)$$

Let the tracking error e_i based on output state response x_i and the desired reference points r_i, be defined as $e_i = x_i - r_i$, where $i = 1, 2, \ldots, n$. Then the fractional order error dynamics can be written as:

$$D^q e_i = D^q x_i - D^q r_i. \qquad (11)$$

In the designing of AFSO-PIDSMC technique, our aim is to design PIDSMC input $u_i(t)$ such that $e_i(t) \to 0$ at $t \to \infty$. Utilising the Caputo's Definition 2 [74], the qth fractional order derivative, discussed in preliminaries, the $(PID)^q$ sliding surface is defined as follows:

$$s_i(t) = \kappa_{Pi}(e_i) + \kappa_{Ii} D^{-q}(e_i) + \kappa_{Di} D^q(e_i), \quad (12)$$

where $q \in (0, 1)$, κ_{Pi}, κ_{Ii}, and κ_{Di} are the proportional, integral and derivative constants for ith dimension dynamics. When $q = 1$, the integer order PID sliding surface can be obtained.

Remark 2 According to the definitions on fractional order calculus discussed in Sect. 2, the integral operator has one additional weight function to that of the integer order integral operator, and the value of additional weight function happens to be large initially and

lowers with increasing time [43]. As a result, response time becomes faster initially, but there is a risk of significant overshoot and a fractional order differential term is required to maintain the significant overshoot and speed of response both.

Using Eqs. (11) and (12), the fractional first and second order sliding surface dynamics can be written as:

$$\begin{cases} D^q s_i = \kappa_{Pi} D^q e_i + \kappa_{Ii} e_i + \kappa_{Di} D^{2q} e_i \\ D^{2q} s_i = \kappa_{Pi} D^{2q} e_i + \kappa_{Ii} D^q e_i + \kappa_{Di} D^{3q} e_i. \end{cases} \qquad (13)$$

SMC law contains two fundamental controls to ensure the system dynamics in the sliding mode, namely equivalent control (u_{eqi}) and switching control (u_{si}). The fractional order system dynamics (10) is in sliding motion, if it satisfies the fractional first and second order sliding surface dynamics as $D^q s_i = 0$ and $D^{2q} s_i = 0$. Utilising sliding mode condition, the adaptive equivalent control laws u_{eqi1} and u_{eqi2} can be written as follows:

$$\begin{cases} u_{eqi1} = -\kappa_{Pi}\left(D^q \hat{x}_i - D^q r_i\right) - \kappa_{Ii}(\hat{x}_i - r_i) \\ \qquad\quad - \kappa_{Di}(D^{2q} \hat{x}_i - D^{2q} r_i) \\ u_{eqi2} = -\kappa_{Pi}\left(D^{2q} \hat{x}_i - D^{2q} r_i\right) - \kappa_{Ii}(D^q \hat{x}_i - D^q r_i) \\ \qquad\quad - \kappa_{Di}(D^{3q} \hat{x}_i - D^{3q} r_i) \end{cases} \qquad (14)$$

where $D^q \hat{X} = f(X, t) + \hat{\gamma}_1 G_1(t) + \hat{\gamma}_2 G_2(t) + \hat{\gamma}_3 D^r(t)$, such that $\hat{\gamma}_1, \hat{\gamma}_2$ are the unknown, bounded amplitudes of two disturbances and $\hat{\gamma}_3$ is the unknown and bounded amplitude of external noise and are considered to be conveniently estimated. Let the parameter estimation error be defined as follows:

$$e_{\gamma_1} = \hat{\gamma}_1 - \gamma_1, \quad e_{\gamma_2} = \hat{\gamma}_2 - \gamma_2, \quad e_{\gamma_3} = \hat{\gamma}_3 - \gamma_3. \qquad (15)$$

The second crucial control law, switching control law, is designed to drive and maintain the fraction order system trajectory on the sliding surface. Let the fractional first and second order switching control laws, u_{si1} and u_{si2}, respectively, be defined as follows:

$$u_{si1} = -\eta_i \, \text{sign}(s_i), \quad u_{si2} = -\eta_{i1} \, \text{sign}(D^q s_i), \quad (16)$$

where η_i and η_{i1} are positive constants. Using equations (14) and (16), the adaptive fractional first and second order net control law is written as:

$$u_i = u_{eqi1} + u_{eqi2} + u_{si1} + u_{si2} \qquad (17)$$

Theorem The fractional order sliding surfaces (13) are asymptotically stable if the adaptive control input $u_i(t)$
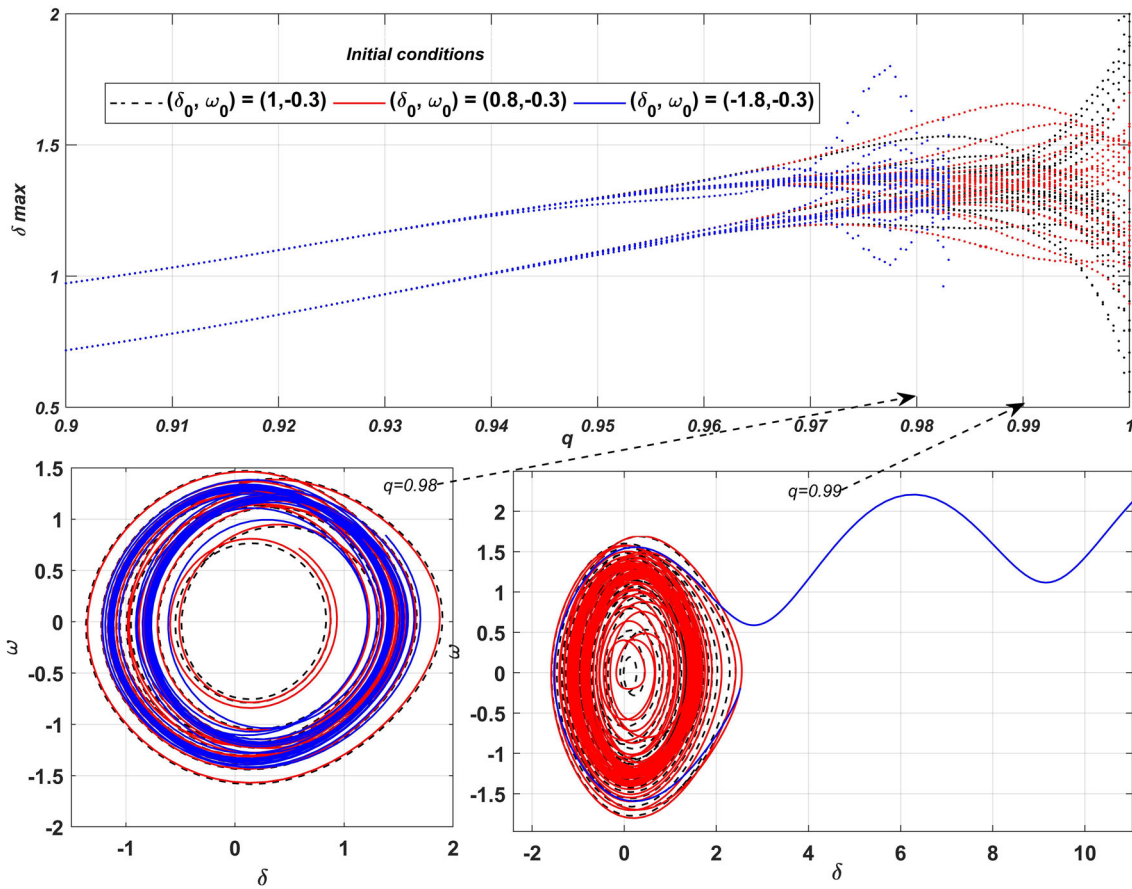
Fig. 11 Coexisting bifurcation diagram of generator rotor angle (δ) and phase portrait with the given three initial conditions when order of fractional derivative (q) is varied
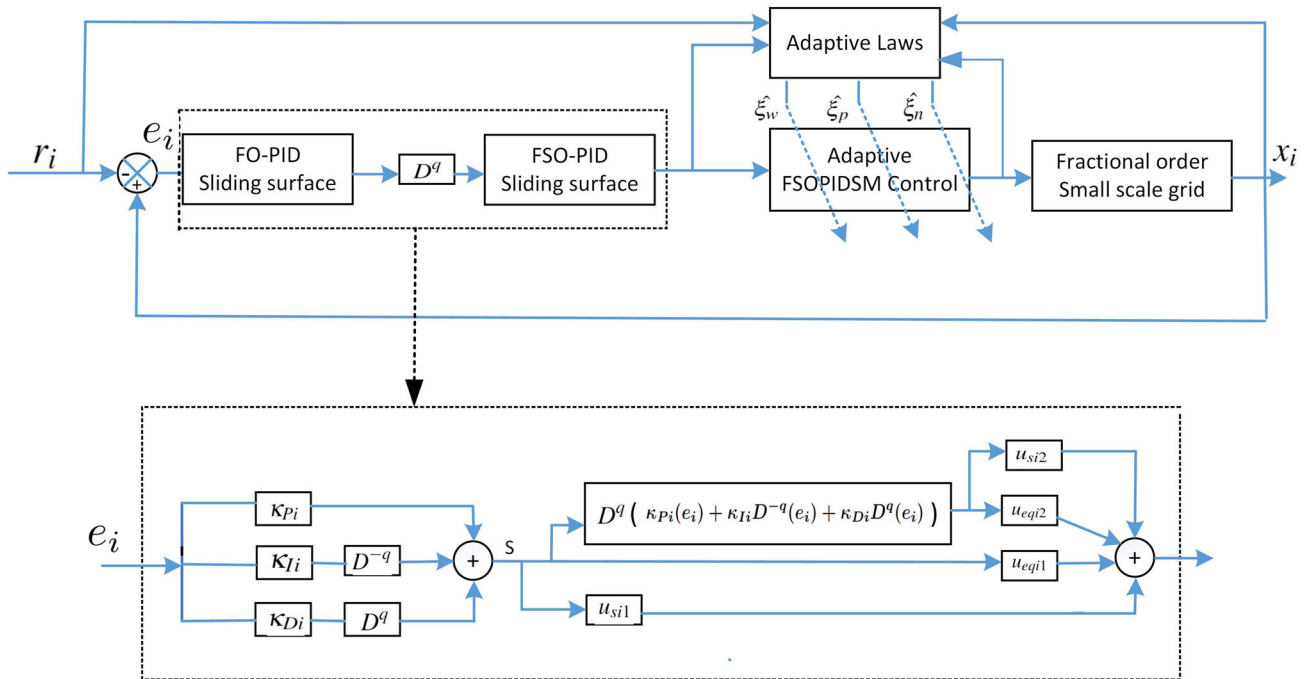
Fig. 12 Close loop block diagram of proposed adaptive fractional second order AFSO-PIDSMC technique

2428

Eur. Phys. J. Spec. Top. (2023) 232:2415–2436

in (17) is applied to the uncertain nonlinear system with external disturbances (10) such that error $e_i \to 0$ as $t \to \infty$ and the parameter estimation law in (18) ensures the adaptation of uncertain/unknown parameters.

$$
\begin{cases}
D^q\hat{\gamma}_1 = k_{Pi}G_1(t) + k_{Di}D^qG_1(t) + D^qs_i.D^qk_{Pi}G_1(t) \\
+ D^qs_i.k_{Di}D^{2q}G_1(t) - h_1(\hat{\gamma}_1 - \gamma_1) \\
D^q\hat{\gamma}_2 = k_{Pi}G_2(t) + k_{Di}D^qG_2(t) + D^qs_i.D^qk_{Pi}G_2(t) \\
+ D^qs_i.k_{Di}D^{2q}G_2(t) - h_2(\hat{\gamma}_2 - \gamma_2) \\
D^q\hat{\gamma}_3 = k_{Pi}D^r(t) + k_{Di}D^qD^r(t) + D^qs_i.D^qk_{Pi}D^r(t) \\
+ D^qs_i.k_{Di}D^{2q}D^r(t) - h_3(\hat{\gamma}_3 - \gamma_3)
\end{cases}
\tag{18}
$$

Proof Let the Lyapunov function candidate be selected as:

$$
V(s_i) = \frac{1}{2}[s_i^2 + (D^qs_i)^2 + (e_{\gamma_1})^2 + (e_{\gamma_2})^2 + (e_{\gamma_3})^2]
\tag{19}
$$

Lemma 1 [48] If $s_i(t)$ is a continuously differential function, then for all $t \geq a$, $\frac{1}{2}{_a}D_t^q s_i^2(t) \leq s_i(t){_a}D_t^q s_i(t)$, $\forall q \in (0, 1]$, where $i = 1, 2, \ldots, N$.

If Lyapunov function candidate (19) satisfies Lemma 1 [48] and *Properties* [74] of fractional order calculus, the fractional derivative of Lyapunov function candidate can be written as follows:

$$
\begin{cases}
D^qV(s_i) \leq s_iD^qs_i + D^qs_i.(D^{2q}s_i) + e_{\gamma_1}D^qe_{\gamma_1} \\
+ e_{\gamma_2}D^qe_{\gamma_2} + e_{\gamma_3}D^qe_{\gamma_3}
\end{cases}
\tag{20}
$$

Using Eqs. (13) and (15) in (20), the fractional derivative of Lyapunov function candidate is written in (21).

$$
\begin{cases}
D^qV(s_i) \leq s_i\{k_{Pi}(D^qx_i) + k_{Di}(D^{2q}x_i) - k_{Pi}(D^q\hat{x}_i) \\
- k_{Di}(D^{2q}\hat{x}_i)\} - s_i\eta_i sign(s_i) + D^qs_i.\{k_{Pi}(D^{2q}x_i) \\
+ \kappa_{Ii}D^qx_i + k_{Di}(D^{3q}x_i) - k_{Pi}(D^{2q}\hat{x}_i) \\
- \kappa_{Ii}D^q\hat{x}_i - k_{Di}(D^{3q}\hat{x}_i)\} \\
- D^qs_i.\eta_{i1}sign(D^qs_i) \\
+ (\hat{\gamma}_1 - \gamma_1)\{D^q\hat{\gamma}_1 + h_1(\hat{\gamma}_1 - \gamma_1)\} + (\hat{\gamma}_2 - \gamma_2)\{D^q\hat{\gamma}_2 \\
+ h_2(\hat{\gamma}_2 - \gamma_2)\} + (\hat{\gamma}_3 - \gamma_3)\{D^q\hat{\gamma}_3 + h_3(\hat{\gamma}_3 - \gamma_3)\}
\end{cases}
\tag{21}
$$

Using control laws (17) in (21), $D^qV(s_i)$ further be simplified as folows:

$$
\begin{cases}
D^qV(s_i) \leq (\hat{\gamma}_1 - \gamma_1)\{-k_{Pi}G_1(t) - k_{Di}D^qG_1(t) \\
- D^qs_i.k_{Pi}D^qG_1(t) - D^qs_i.k_{Di}D^{2q}G_1(t) \\
\quad + D^q\hat{\gamma}_1 \\
+ h_1(\hat{\gamma}_1 - \gamma_1)\} + (\hat{\gamma}_2 - \gamma_2) \\
\{-k_{Pi}G_2(t) - k_{Di}D^qG_2(t) - D^qs_i.k_{Pi}D^qG_2(t) \\
\quad - D^qs_i.k_{Di}D^{2q}G_2(t) \\
+ D^q\hat{\gamma}_2 + h_2(\hat{\gamma}_2 - \gamma_2)\} + (\hat{\gamma}_3 - \gamma_3) \\
\{-k_{Pi}D^r(t) - k_{Di}D^qD^r(t) \\
\quad - D^qs_i.k_{Pi}D^qD^r(t) - D^qs_i.k_{Di}D^{2q}D^r(t) \\
+ D^q\hat{\gamma}_3 + h_3(\hat{\gamma}_3 - \gamma_3)\} - \eta_i s_i \ sign(s_i) \\
\quad - \eta_{i1}(D^qs_i)sign(D^qs_i)
\end{cases}
\tag{22}
$$

Further, using the parameter estimation laws (18) in the fractional derivative of Lyapunov function $D^qV(s_i)$ in (22) results the following negative semi-definite expression.

$$
D^qV(s_i) \leq -\eta_i s_i \ sign(s_i) - \eta_{i1}(D^qs_i)sign(D^qs_i),
\tag{23}
$$

where η_i, η_{i1} are positive constants. $D^qV(s_i) < 0 \ \forall \ s_i$, $D^qs_i \neq 0$, confirms that the fractional order sliding surface is asymptotically stable and the error converges asymptotically.

In the next section, control of chaos and multistability behaviours in the fractional order SSG system using the AFSO-PIDSMC technique is discussed.

5.1 AFSO-PIDSMC of chaos and multistability behaviours in the fractional order SSG

The AFSO-PIDSMC technique is employed to control the fractional order SSG with uncertainties and disturbances. The fractional order small scale grid dynamics (8) with added control can be written as follows:

$$
\begin{cases}
D^q\delta = \omega + u_1 \\
D^q\omega = \sigma - \rho\sin\delta - \lambda\omega + \xi_w\cos(\beta_1 t) + \xi_p\cos(\beta_2 t) + \xi_n\gamma(t) + u_2
\end{cases}
\tag{24}
$$

The Eq. (24) may be related in term of equation (9) as:
$$
D^qX = \begin{bmatrix} {_a}D_t^q\delta \\ {_a}D_t^q\omega \end{bmatrix}, \ f(X, t) = \begin{bmatrix} \omega \\ \sigma - \rho\sin\delta - \lambda\omega \end{bmatrix}, \ \gamma_1 =
$$

ξ_w, $G_1(t) = \begin{bmatrix} 0 \\ cos(\beta_1 t) \end{bmatrix}$, $\gamma_2 = \xi_p$, $G_2(t) = \begin{bmatrix} 0 \\ cos(\beta_2 t) \end{bmatrix}$, $\gamma_3 = \xi_n$, $D^r(t) = \begin{bmatrix} 0 \\ \gamma(t) \end{bmatrix}$, and $u_i = \begin{bmatrix} u_1 \\ u_2 \end{bmatrix}$.

Let the tracking error be defined as $[e_1; \ e_2] = [\delta - \delta^*; \ \omega - \omega^*]$, where δ, ω represent the state variables. δ^*, ω^* are the desired values of fractional order SSG system; then fractional order error dynamics is written as follows:

$$D^q e_1 = D^q \delta - D^q \delta^*, \quad D^q e_2 = D^q \omega - D^q \omega^* \tag{25}$$

The qth order PID sliding surfaces s_1, s_2 are defined as per Eq. (12) and the fractional first and second-order sliding surface dynamics are written in (26) and (27), respectively.

$$\begin{cases} D^q s_1 = \kappa_{P1} (D^q \delta - D^q \delta^*) + \kappa_{I1}(\delta - \delta^*) + \kappa_{D1}(D^{2q}\delta - D^{2q}\delta^*) \\ D^q s_2 = \kappa_{P2} (D^q \omega - D^q \omega^*) + \kappa_{I1}(\omega - \omega^*) + \kappa_{D2}(D^{2q}\omega - D^{2q}\omega^*) \end{cases} \tag{26}$$

$$\begin{cases} D^{2q} s_1 = \kappa_{P1} (D^{2q}\delta - D^{2q}\delta^*) + \kappa_{I1}(D^q\delta - D^q\delta^*) + \kappa_{D1}(D^{3q}\delta - D^{3q}\delta^*) \\ D^{2q} s_2 = \kappa_{P2} (D^{2q}\omega - D^{2q}\omega^*) + \kappa_{I2}(D^q\omega - D^q\omega^*) + \kappa_{D2}(D^{3q}\omega - D^{3q}\omega^*) \end{cases} \tag{27}$$

The fractional second-order sliding surfaces satisfy the sliding motion conditions as $D^q s_i = 0$ and $D^{2q} s_i = 0$, and based on (13), the adaptive equivalent control laws; $u_{eq11} + u_{eq12}$ for sliding surface s_1 and $u_{eq21} + u_{eq22}$ for sliding surface s_2, are written in (28).

$$\begin{cases} u_{eq11} + u_{eq12} = -\kappa_{P1} (D^q\hat{\delta} - D^q\delta^*) - \kappa_{I1}(\delta - \delta^*) \\ \quad -\kappa_{D1}(D^{2q}\hat{\delta} - D^{2q}\delta^*) - \kappa_{P1} (D^{2q}\hat{\delta} - D^{2q}\delta^*) \\ \quad -\kappa_{I1}(D^q\hat{\delta} - D^q\delta^*) - \kappa_{D1}(D^{3q}\hat{\delta} - D^{3q}\delta^*) \\ u_{eq21} + u_{eq22} = -\kappa_{P2} (D^q\hat{\omega} - D^q\omega^*) - \kappa_{I1}(\omega - \omega^*) \\ \quad -\kappa_{D2}(D^{2q}\hat{\omega} - D^{2q}\omega^*) - \kappa_{P2} (D^{2q}\hat{\omega} - D^{2q}\omega^*) \\ \quad -\kappa_{I2}(D^q\hat{\omega} - D^q\omega^*) - \kappa_{D2}(D^{3q}\hat{\omega} - D^{3q}\omega^*,) \end{cases} \tag{28}$$

where $D^q\hat{\delta} = \omega$, and $D^q\hat{\omega} = \sigma - \rho sin\delta - \lambda\omega + \hat{\xi}_w cos(\beta_1 t) + \hat{\xi}_p cos(\beta_2 t) + \hat{\xi}_n \gamma(t)$. $\hat{\xi}_w$, $\hat{\xi}_p$ are the unknown amplitudes of random wind power and periodic load, respectively, referred to as disturbances, and $\hat{\xi}_n$ is the unknown amplitude of external noise intensity, are to be estimated. Then, with reference to (14), the param-

eter estimation error is defined as $e_{\gamma_1} = e_{\xi_w} = \hat{\xi}_w - \xi_w$, $e_{\gamma_2} = e_{\xi_p} = \hat{\xi}_p - \xi_p$, and $e_{\gamma_3} = e_{\xi_n} = \hat{\xi}_n - \xi_n$. Similarly, as per the Eq. (16), the switching control law for first and second orders is written as follows:

$$\begin{cases} u_{s11} + u_{s12} = -\eta_1 \ sign(s_1) - \eta_{11} \ sign(D^q s_1) \\ u_{s21} + u_{s22} = -\eta_2 \ sign(s_2) - \eta_{21} \ sign(D^q s_2). \end{cases} \tag{29}$$

Further, using Eqs. (28) and (29), the net control laws can be obtained as:

$$\begin{cases} u_1 = u_{eq11} + u_{eq12} + u_{s11} + u_{s12} \\ u_2 = u_{eq21} + u_{eq22} + u_{s21} + u_{s22}. \end{cases} \tag{30}$$

As per definition of Theorem and its proof, the designed adaptive second-order PIDSMC laws in (30) and the parameter estimation laws in (31) ensure the asymptotic stability of sliding surfaces and estimation of unknown parameters such as disturbances and noise.

$$\begin{cases} D^q\hat{\xi}_w = s_2.k_{P2}.cos(\beta_1 t) + s_2.k_{D2}.D^q cos(\beta_1 t) + D^q s_2.k_{P2} \\ \quad .D^q cos(\beta_1 t) + D^q s_2.k_{D2}.D^{2q} cos(\beta_1 t) - h_1(\hat{\xi}_w - \xi_w) \\ D^q\hat{\xi}_p = k_{P2}.cos(\beta_2 t) + k_{D2}.D^q cos(\beta_2 t) + D^q s_2.k_{P2} \\ \quad .D^q cos(\beta_2 t) + D^q s_2.k_{D2}.D^{2q} cos(\beta_2 t) - h_2(\hat{\xi}_p - \xi_p) \\ D^q\hat{\xi}_n = k_{P2}.\gamma(t) + k_{D2}.D^q\gamma(t) + D^q s_2.k_{P2}.D^q\gamma(t) \\ \quad + D^q s_2.k_{D2}.D^{2q}\gamma(t) - h_3(\hat{\xi}_n - \xi_n). \end{cases} \tag{31}$$

Moreover, the selected Lyapunov function candidate is given in (32) and the obtained $D^q V(s)$ is written in (34) for the sake of clarity.

$$V(s) = \frac{1}{2}[s_1^2 + (D^q s_1)^2 + s_2^2 + (D^q s_2)^2 + e_{\xi_w}^2 + e_{\xi_p}^2 + e_{\xi_n}^2]. \tag{32}$$

If Lyapunov function candidate (32) satisfies Lemma 1 [48] and Properties [74] of fractional order calculus, the fractional derivative of Lyapunov function candidate can be written as follows:

$$D^q V(s_i) \leq s_i D^q s_i + D^q s_i.(D^{2q} s_i) + e_{\gamma_1} D^q e_{\gamma_1} + e_{\gamma_2} D^q e_{\gamma_2} + e_{\gamma_3} D^q e_{\gamma_3}. \tag{33}$$

Substituting the Eqs. (25), (26) and (27) in (33) and further written as,

2430

Eur. Phys. J. Spec. Top. (2023) 232:2415–2436

$$
\begin{cases}
D^q V(s) \leq s_1\{k_{P1}(D^q\delta) + k_{D1}(D^{2q}\delta) \\
\quad -k_{P1}(D^q\hat{\delta}) - k_{D1}(D^{2q}\hat{\delta})\} - s_1\eta_1 Sign(s_1) \\
\quad +D^q s_1.\{k_{P1}(D^{2q}\delta) \\
\qquad +\kappa_{I1}D^q\delta + k_{D1}(D^{3q}\delta) \\
\quad -k_{P1}(D^{2q}\hat{\delta}) - \kappa_{I1}D^q\hat{\delta} \\
\quad -k_{D1}(D^{3q}\hat{\delta})\} - D^q s_1.\eta_{11} Sign(D^q s_1) \\
\qquad +s_2\{k_{P2}(D^q\omega) + k_{D2}(D^{2q}\omega) \\
\quad -k_{P2}(D^q\hat{\omega}) - k_{D2}(D^{2q}\hat{\omega})\} - s_2\eta_2 Sign(s_2) \\
\quad +D^q s_2.\{k_{P2}(D^{2q}\omega) \\
\qquad +\kappa_{I2}D^q\omega + k_{D2}(D^{3q}\omega) \\
\quad -k_{P2}(D^{2q}\hat{\omega}) \\
\quad -\kappa_{I2}D^q\hat{\omega} - k_{D2}(D^{3q}\hat{\omega})\} \\
\quad -D^q s_2.\eta_{21} Sign(D^q s_2) \\
\qquad +(\hat{\xi_w} - \xi_w)\{D^q\hat{\xi_w} + h_1(\hat{\xi_w} - \xi_w)\} + (\hat{\xi_p} - \xi_p) \\
\{D^q\hat{\xi_p} + h_2(\hat{\xi_p} - \xi_p)\} + (\hat{\xi_n} - \xi_n) \\
\{D^q\hat{\xi_n} + h_3(\hat{\xi_n} - \xi_n)\}
\end{cases}
\tag{34}
$$

Using the parameter estimation laws (31) in (34), the fractional derivative of Lyapunov function candidate $D^q V(s)$ is further simplified as:

$$
D^q V(s) < -\eta_1|s_1| - \eta_{11}|D^q s_1| - \eta_2|s_2| - \eta_{21}|D^q s_2|,
\tag{35}
$$

for all s_1, $s_2 \neq 0$ and η_1, η_{11}, η_2 and η_{21} are positive constants. Therefore, the fractional order sliding surface is asymptotically stable and the tracking error $e_i \to 0$ at $t \to \infty$ are achieved based on the asymptotic estimation of unknown parameters.

Remark 3 It may be noted that as the fractional order SSG system exhibits irregular (chaos, unstable), multistability behaviours based on rotor angle and frequency oscillations, indicating that the synchronous generators may lose synchronism and the fractional order SSG system may endure severe frequency swings due to power disturbance. In this case, if no significant counter measures are taken to suppress such irregular behaviours, the fractional order SSG system would be in crisis situation resulting a devastating blackout. Therefore, the proposed AFSO-PIDSMC may be useful as a counter measure to control unwanted chaos and multistability behaviours.

## 5.2 Simulation results on control of chaos and multistability

Numerical simulation is done in MATLAB environment and presented to verify the effectiveness of the proposed AFSO-PIDSMC technique. Simulation results for control of chaos and multistability behaviours of the qth fractional order SSG system (8) are presented. When the fractional order $0.98 \leq q < 1$, fractional order SSG system (8) exhibits chaos behaviour which may be referred via bifurcation and phase portrait diagrams shown in Fig. 2d, e.

The state behaviours of fractional order SSG system (8) without and with AFSO-PIDSMC input (30) are presented in Fig. 13, where (a) shows the time series of generator rotor angle (δ) and Fig. 13c shows angular velocity (ω) without control till $t < 150$ s and reflect chaotic behaviour. Once the control is activated at $t = 150$ s, the unwanted chaos behaviour is controlled, estimation the unknown disturbances $\hat{\xi_w} = 0.2$, $\hat{\xi_p} = 0.1$, and noise $\hat{\xi_n} = 0.01$ are achieved successfully as shown in Fig. 14. The designed sliding surfaces, and required control input along with the proposed AFSO-PIDSMC performance in terms of errors are illustrated in Fig. 15 for $T = 150$–160 s (controller is active at $T = 150$ s). It is observed that the designed sliding surfaces are stable and control inputs do not have unwanted chattering. Simultaneously, after the transient time, the zero steady state error confirms that the proposed control technique successfully converges fast to the desired trajectory within 0.25–0.3 s. Furthermore, the proposed control technique is compared with recently published robust-adaptive fractional-order sliding mode control (RAFOSMC) [73] technique and the obtained controlled state responses are shown in Fig. 13b, d, labelled via blue colour, have better and faster tracking performance than the RAFOSMC [73] technique. The value of different parameters are used considered as $\kappa_{p1} = \kappa_{p2} = 1$, $\kappa_{I1} = \kappa_{I2} = 0.15$, $\kappa_{D1} = \kappa_{D2} = 0.15$, $\eta_1 = 0.002$, $\eta_2 = 0.001$, $\eta_{11} = 0.02$, $\eta_{21} = 0.01$, $h_1 = h_2 = h_3 = 5$.

Further, the proposed AFSO-PIDSMC technique is also able to control the multistability behaviour with the same value of control parameters and the results are shown in Fig. 14. In the Fig. 14, multistability of chaotic time series behaviour of generator rotor angle (δ) with three different initial conditions $[\delta_0; \omega_0] = [1; -0.3]$, $[6; -0.3]$, and $[-6.1; -0.3]$ are presented with blue, red and black colours, respectively. When the control is applied at $t = 150s$, it successfully control the multistability behaviour alongside chaos suppression at the desired operating point $\delta = 0.6$. Therefore, the presented results verify the effectiveness and importance of the proposed AFSO-PIDSMC technique as (i) to control of chaos and multistability behaviours in the fractional order SSG, (ii) to avoid the rotor angle instabilities of the fractional order SSG, (iii) provides significant preventive measure in suppressing the irregular behaviours to restrict the SSG system not to fall in
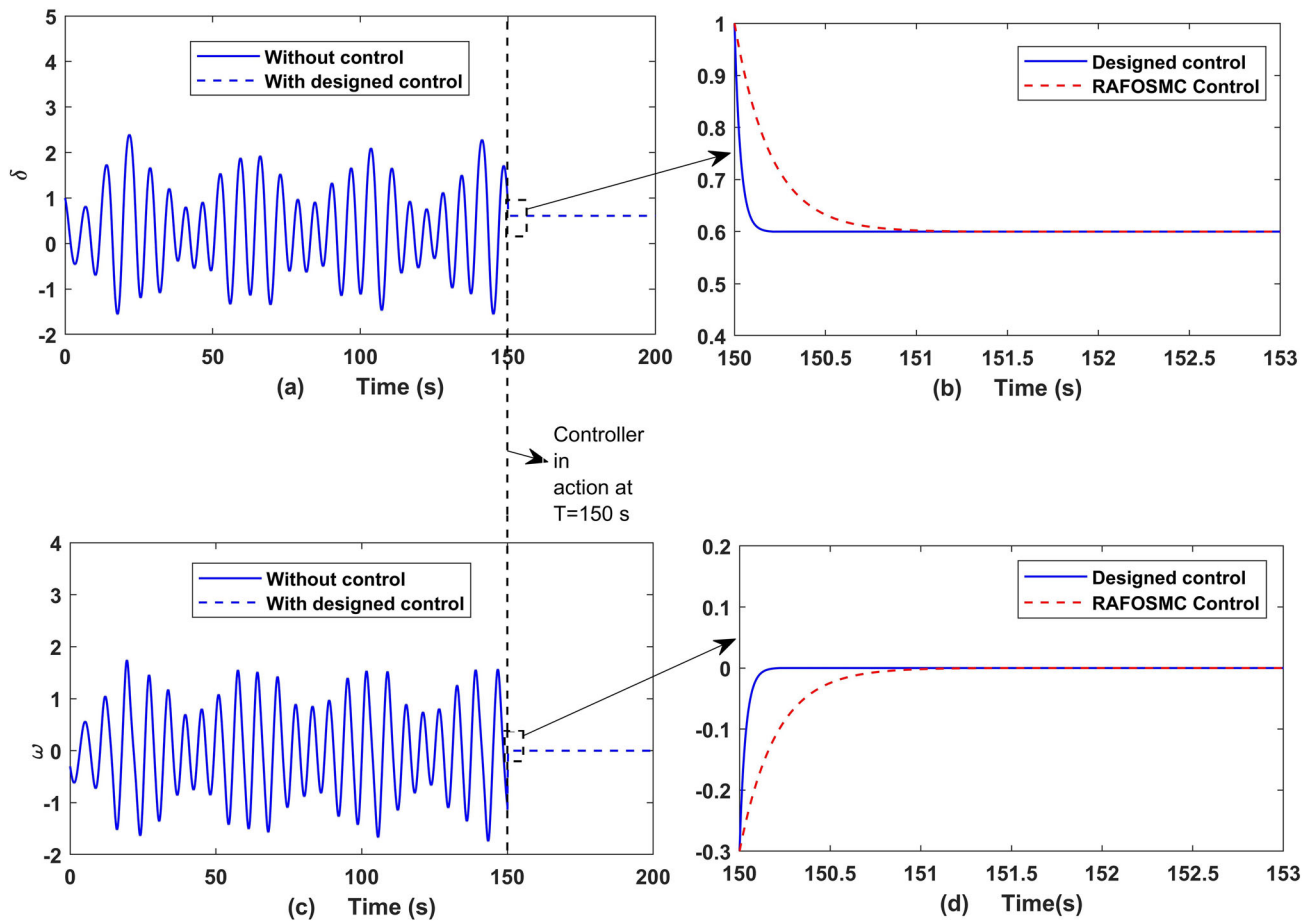
Fig. 13 Control of chaotic behaviour of the rotor angle, angular velocity of synchronous generator and comparison with RAFOSMC [73]
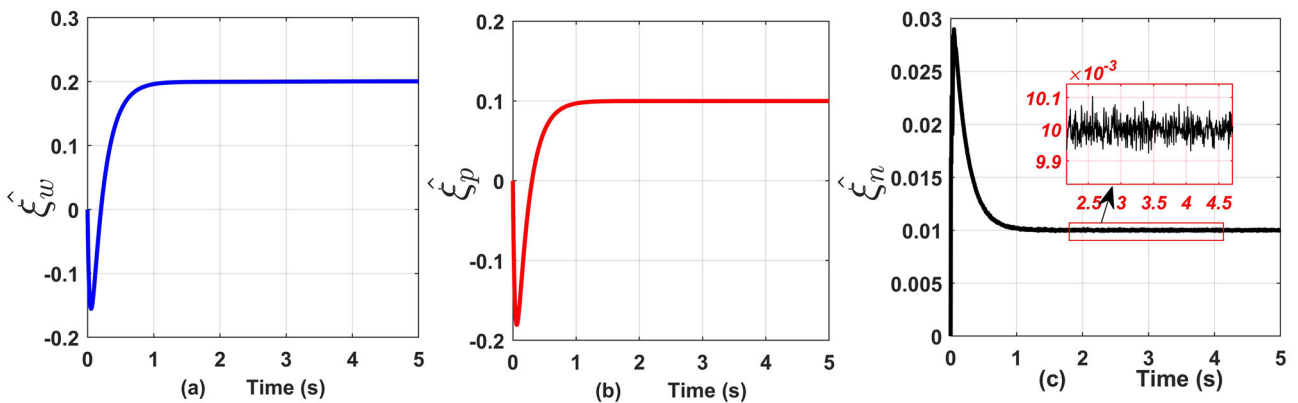
Fig. 14 Adaptive estimation of unknown disturbances and noise parameters of the fractional order SSG (8)

crisis situation via sliding surfaces and control efforts shown in Fig. 16.

In the proposed ASO-PIDSMC technique, the controller is simulated for fractional order $q = 0.98$ in line with fractional order modeling of SSG system to control the chaotic and multistability behaviours. Selection of a fractional order of the controller as $q = 0.98$, effectively controls the presence of chaotic and multistability behaviours. If the actual SSG model is not fractional, it means the system follows traditional calculus principles, i.e., an integer order SSG model. In our past study, the chaos and multistability behaviour have been explored in the integer order SSG system [11] and may be referred for detailed analysis.
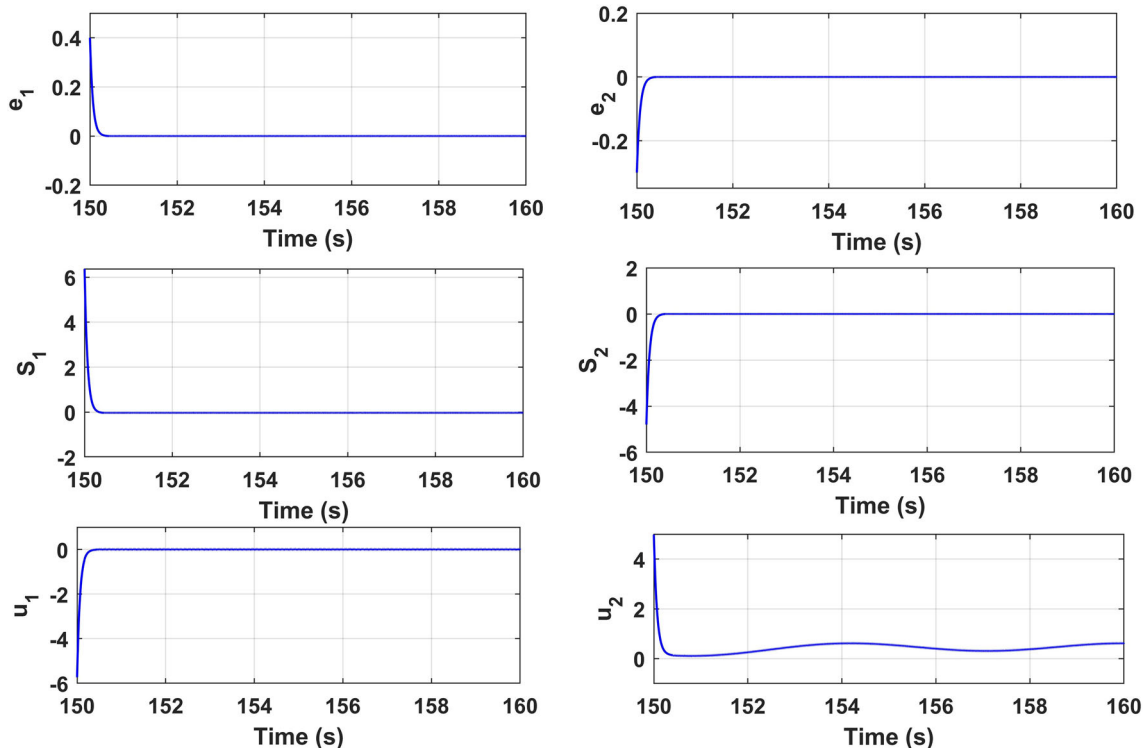
2432

Eur. Phys. J. Spec. Top. (2023) 232:2415–2436

Fig. 15 Errors, AFSO-PID sliding surfaces and control inputs (controller is active at $T = 150$ s)
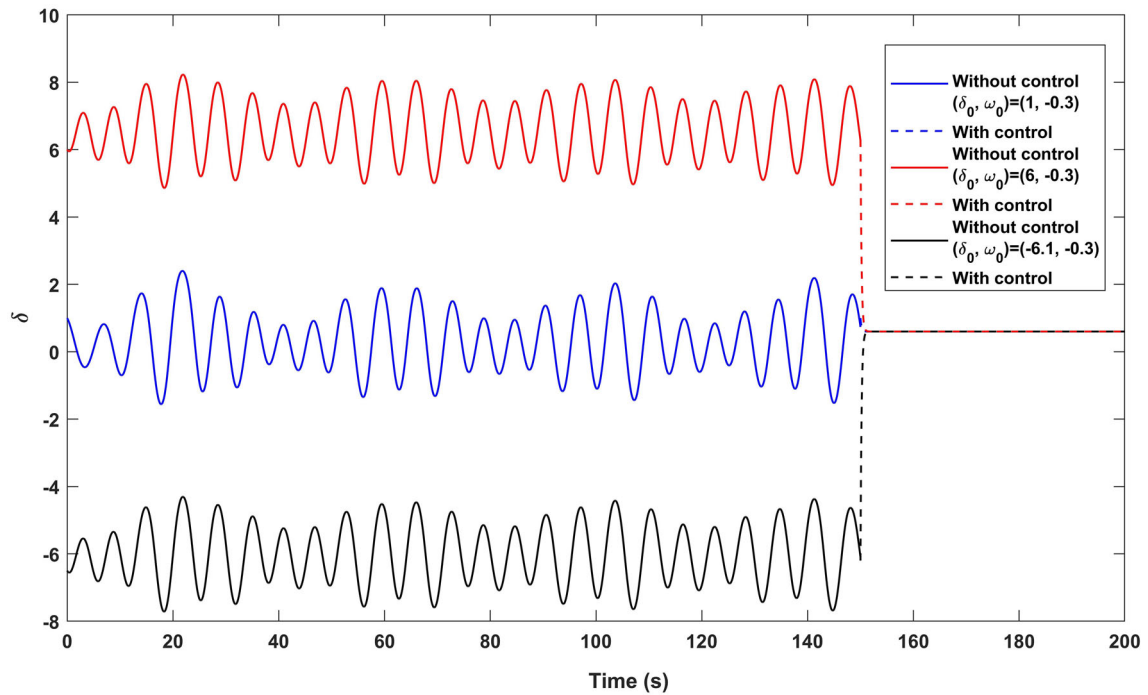

Fig. 16 Control of multistability behaviour of the fractional order SSG system (8) using AFSO-PIDSMC technique

6 Conclusion

In this paper, Caputo's fractional order based small scale grid (SSG) model is explored and studied under the influence of disturbances and external noise. Random wind power and load demand are considered as disturbances, while additive white Gaussian noise (AWGN) is treated as external noise. Different nonlinear dynamical behaviours, classified as regular (periodic), and irregular (chaos, unstable) and PDB route to chaos behaviours, are examined in the fractional order $q \in [0.9, 1)$, varying electromagnetic power $\rho \in [0.9, 1.2]$ and under the presence of varying amplitude of disturbances and noise. Presence of irregular behaviours have substantial impact the fractional order SSG. Bifurcation analysis and corresponding calculated Lyapunov exponents or maximum Lyapunov exponents uncover multiple normal and abnormal behaviours of rotor dynamics under the specific range of varied parameters. The fascinating phenomena; coexisting attractors and multistability are exposed with the change in initial condition and variation in parameters of fraction order SSG dynamics. It is evident that multistability or coexisting behaviours can frequently change the system state from desirable operating point to undesirable or unstable operating point. This creates stability problem in the power system.

An adaptive control based on the design of fractional second order PID sliding mode control strategy, known as AFSO-PIDSMC technique, is proposed to control the chaos and multistability behaviours and is compared with robust adaptive fractional order sliding mode control (RAFOSMC) [73] technique. The proposed AFSO-PIDSMC has faster tracking speed and estimation of unknown parameters. The entire simulations are accomplished in MATLAB environment and effectively verify the complete system and control analyses.

The fractional order SSG dynamics under study provides new insights to tackle multistability and coexisting behaviours compared to existing research [9–11, 13] and useful in redefining a new counter measure for such undesirable dynamic irregularities. The findings on the fractional order SSG system and control under study will help to improve the knowledge (i) to understand the complicated nonlinear dynamic behaviours and (ii) to eliminate the presence of multistability and coexistence behaviours in power grids.

In our opinion, the fractional order derivative should match both in the modeling and control. If the fractional order is different in either case, implementation issues may arise during real time scenario. However, this is still open as a contemporary debatable topic for researchers. Finally, the present study and control may be utilised in the large scale or complex power grid, since multistability or coexisting behaviours create serious problem of global stability in the large scale or complex power grid network and control of multistability becomes a challenging task and researchers may explore in future.

Author contribution statement

PCG methodology; formal analysis; software; writing-original draft. PP conceptualization; supervision; validation; writing/editing-original draft.

Data availability The data that supports the findings of this study are available within the article.

Declarations

Conflict of interest The authors have no conflicts to disclose.

References

1. P.C. Gupta, A. Banerjee, P.P. Singh, Analysis and control of chaotic oscillation in FOSMIB power system using AISMC technique, in *2019 IEEE Students Conference on Engineering and Systems (SCES), Allahabad, India*, pp. 1–6 (2019). https://doi.org/10.1109/SCES46477.2019.8977223. https://ieeexplore.ieee.org/document/8977223/. Accessed 11 June 2021

2. P. Das, P.C. Gupta, P.P. Singh, Bifurcation, chaos and PID sliding mode control of 3-bus power system, in *2020 3rd International Conference on Energy, Power and Environment: Towards Clean Energy Technologies, Shillong, Meghalaya, India*, pp. 1–6 (2021). https://doi.org/10.1109/ICEPE50861.2021.9404493. https://ieeexplore.ieee.org/document/9404493/. Accessed 25 Sept 2022

3. H.K. Chen, T.N. Lin, J.H. Chen, Dynamic analysis, controlling chaos and chaotification of a smib power system. Chaos Solitons Fractals **22**, 1307–1315 (2005)

4. Y. Yu, H. Jia, P. Li, J. Su, Power system instability and chaos. Electr. Power Syst. Res. **65**(3), 187–195 (2003). https://doi.org/10.1016/S0378-7796(02)00229-8

5. P.C. Gupta, A. Banerjee, P.P. Singh, Analysis of global bifurcation and chaotic oscillation in distributed generation integrated novel renewable energy system, in *2018 15th IEEE India Council International Conference (INDICON), pp. 1–5. IEEE, Coimbatore, India* (2018). https://doi.org/10.1109/INDICON45594.2018.8986983. https://ieeexplore.ieee.org/document/8986983/. Accessed 21 June 2023

6. C.V. Nayar, Recent developments in decentralised mini-grid diesel power systems in Australia. Appl. Energy **52**(2–3), 229–242 (1995). https://doi.org/10.1016/0306-2619(95)00046-U

7. M. Gujar, A. Datta, P. Mohanty, Smart mini grid: an innovative distributed generation based energy system, in *2013 IEEE Innovative Smart Grid Technologies-Asia (ISGT Asia)*, pp. 1–5 (2013). https://doi.org/10.1109/ISGT-Asia.2013.6698768

8. M. Saleh, Y. Esa, Y. Mhandi, W. Brandauer, A. Mohamed, Design and implementation of CCNY DC microgrid testbed, in *2016 IEEE Industry Applications*

2434

Eur. Phys. J. Spec. Top. (2023) 232:2415–2436

Society Annual Meeting, Portland, USA, pp. 1–7 (2016). https://doi.org/10.1109/IAS.2016.7731870. http://ieee xplore.ieee.org/document/7731870/. Accessed 25 Sept 2022

9. Y.H. Qin, J.C. Li, Random parameters induce chaos in power systems. Nonlinear Dyn. **77**, 1609–1615 (2014)

10. X. Wang, Y. Chen, G. Han, C. Song, Nonlinear dynamic analysis of a single-machine infinite-bus power system. Appl. Math. Model. **39** (2015)

11. P.C. Gupta, P.P. Singh, Chaos, multistability and coexisting behaviours in small-scale grid: impact of electromagnetic power, random wind energy, periodic load and additive white Gaussian noise. Pramana **97**(1), 3 (2022). https://doi.org/10.1007/s12043-022-02478-w

12. Y. Susuki, I. Mezic, T. Hikihara, Coherent swing instability of power grids. J. Nonlinear Sci. **21**, 403–439 (2011). https://doi.org/10.1007/s00332-010-9087-5

13. K.S. Suchithra, E.A. Gopalakrishnan, J. Kurths, E. Surovyatkina, Emergency rate-driven control for rotor angle instability in power systems. Chaos Interdiscip. J. Nonlinear Sci. **32**, 061102 (2022). https://doi.org/10.1063/5.0093450

14. A.P. Lerm, C.A. Canizares, Multiparameter bifurcation analysis of the south Brazilian power system. IEEE Trans. Power Syst. **18**, 737–746 (2003)

15. H.-D. Chiang, I. Dobson, R.J. Thomas, J.S. Thorp, L. Fekih-Ahmedr, On voltage collapse in electric power systems. IEEE Trans. Power Syst. **5**, 601–611 (1990)

16. D.Q. Wei, X.S. Luo, Noise-induced chaos in single-machine infinite-bus power systems. Eur. Phys. Lett. **86**, 50008 (2009)

17. L. Zhou, F. Chen, Chaotic dynamics for a class of single-machine-infinite bus power system. J. Vib. Control **24**(3), 582–587 (2016). https://doi.org/10.1177/1077546316645225

18. D. Chen, S. Liu, X. Ma, Modeling, nonlinear dynamical analysis of a novel power system with random wind power and it's control. Energy **53**, 139–146 (2013). https://doi.org/10.1016/j.energy.2013.02.013

19. X. Wang, Z. Lu, C. Song, Chaotic threshold for a class of power system model. Shock Vib. **2019**, 1–7 (2019). https://doi.org/10.1155/2019/3479239

20. X. Wang, Y. Chen, L. Hou, Nonlinear dynamic singularity analysis of two interconnected synchronous generator system with 1:3 internal resonance and parametric principal resonance. Appl. Math. Mech. (2015). https://doi.org/10.1007/s10483-015-1965-7

21. H. Zhang, K. Sun, S. He, A fractional-order ship power system with extreme multistability. Nonlinear Dyn. **106**, 1027–1040 (2021)

22. V. Ghaffari, A. Razminia, M. Mirzaei, Improved robust adaptive control law for a class of uncertain nonlinear systems and its application to chaotic systems. Iran. J. Sci. Technol. Trans. Electr. Eng. **43**(4), 741–756 (2019). https://doi.org/10.1007/s40998-019-00194-7

23. A. Giakoumis, C. Volos, A.J.M. Khalaf, A. Bayani, I. Stouboulos, K. Rajagopal, S. Jafari, Analysis, synchronization and microcontroller implementation of a new quasiperiodically forced chaotic oscillator with megastability. Iran. J. Sci. Technol. Trans. Electr. Eng. **44**(1), 31–45 (2020). https://doi.org/10.1007/s40998-019-00232-4

24. S. Çiçek, U.E. Kocamaz, Y. Uyaroğlu, Secure chaotic communication with jerk chaotic system using sliding mode control method and its real circuit implementation. Iran. J. Sci. Technol. Trans. Electr. Eng. **43**(3), 687–698 (2019). https://doi.org/10.1007/s40998-019-00184-9

25. B. Bao, M. Chen, H. Bao, X. Quan, Extreme multistability in a memristive circuit. Electron. Lett. (2016). https://doi.org/10.1049/el.2016.0563

26. M. Tuna, A. Karthikeyan, K. Rajagopal, M. Alcin, S. Koyuncu, Hyperjerk multiscroll oscillators with megastability: analysis, FPGA implementation and a novel ANN-ring-based true random number generator. AEU Int. J. Electron. Commun. **112**, 152941 (2019). https://doi.org/10.1016/j.aeue.2019.152941

27. P. Prakash, K. Rajagopal, J.P. Singh, B.K. Roy, Megastability in a quasi-periodically forced system exhibiting multistability, quasi-periodic behaviour, and its analogue circuit simulation. AEU Int. J. Electron. Commun. **92**, 111–115 (2018). https://doi.org/10.1016/j.aeue.2018.05.021

28. V. Sundarapan, R. Karthikeya, Anti-synchronization of Lu and Pan chaotic systems by adaptive nonlinear control. Int. J. Soft Comput. **6**(4), 111–118 (2011). https://doi.org/10.3923/ijscomp.2011.111.118

29. P.C. Gupta, P.P. Singh, Multistability, multiscroll chaotic attractors and angle instability in multi-machine swing dynamics. IFAC-PapersOnLine **55**(1), 572–578 (2022). https://doi.org/10.1016/j.ifacol.2022.04.094

30. J. Cao, C. Ma, Z. Jiang, S. Liu, Nonlinear dynamic analysis of fractional order rub-impact rotor system. Commun. Nonlinear Sci. Numer. Simul. **16**(3), 1443–1463 (2011). https://doi.org/10.1016/j.cnsns.2010.07.005

31. I. Petráš, R.L. Magin, Simulation of drug uptake in a two compartmental fractional model for a biological system. Commun. Nonlinear Sci. Numer. Simul. **16**(12), 4588–4595 (2011). https://doi.org/10.1016/j.cnsns.2011.02.012

32. K. Rajagopal, A. Karthikeyan, A. Srinivasan, Dynamical analysis and FPGA implementation of a chaotic oscillator with fractional-order memristor components. Nonlinear Dyn. **91**(3), 1491–1512 (2018). https://doi.org/10.1007/s11071-017-3960-9

33. K. Rajagopal, C. Li, F. Nazarimehr, A. Karthikeyan, P. Duraisamy, S. Jafari, Chaotic dynamics of modified wien bridge oscillator with fractional order memristor. Radioengineering 27(1), 165–174 (2019). https://doi.org/10.13164/re.2019.0165

34. M.K. Shukla, B.B. Sharma, Stabilization of a class of fractional order chaotic systems via backstepping approach. Chaos Solitons Fractals **98**, 56–62 (2017). https://doi.org/10.1016/j.chaos.2017.03.011

35. M.K. Shukla, B.B. Sharma, Stabilization of a class of uncertain fractional order chaotic systems via adaptive backstepping control, in *2017 Indian Control Conference (ICC), pp. 462–467. IEEE, Guwahati, India* (2017). https://doi.org/10.1109/INDIANCC.2017.7846518. http://ieeexplore.ieee.org/document/7846518/. Accessed 21 June 2023

36. M.K. Shukla, B.B. Sharma, Stabilization of fractional order discrete chaotic systems, in *Fractional Order Control and Synchronization of Chaotic Systems*, ed. by A.T. Azar, S. Vaidyanathan, A. Ouannas, vol.

688, pp. 431–445. Springer, Cham (2017). https://doi.org/10.1007/978-3-319-50249-6_14. http://link.springer.com/10.1007/978-3-319-50249-6_14. Accessed 21 June 2023

37. M.K. Shukla, B.B. Sharma, Backstepping based stabilization and synchronization of a class of fractional order chaotic systems. Chaos Solitons Fractals **102**, 274–284 (2017). https://doi.org/10.1016/j.chaos.2017.05.015

38. M.K. Shukla, B.B. Sharma, Investigation of chaos in fractional order generalized hyperchaotic Henon map. AEU Int. J. Electron. Commun. **78**, 265–273 (2017). https://doi.org/10.1016/j.aeue.2017.05.009

39. M.K. Shukla, B.B. Sharma, Control and synchronization of a class of uncertain fractional order chaotic systems via adaptive backstepping control: control and synchronization of uncertain fractional order chaotic systems. Asian J. Control **20**(2), 707–720 (2018). https://doi.org/10.1002/asjc.1593

40. M.A. Ezzat, Theory of fractional order in generalized thermoelectric MHD. Appl. Math. Model. **35**(10), 4965–4978 (2011). https://doi.org/10.1016/j.apm.2011.04.004

41. V. Gafiychuk, B. Datsko, V. Meleshko, Mathematical modeling of time fractional reaction-diffusion systems. J. Comput. Appl. Math. **220**(1–2), 215–225 (2008)

42. F. Sun, Q. Li, Dynamic analysis and chaos of the 4D fractional-order power system. Abstr. Appl. Anal. **2014**, 1–8 (2014). https://doi.org/10.1155/2014/534896

43. J. Ni, L. Liu, C. Liu, X. Hu, Fractional order fixed-time nonsingular terminal sliding mode synchronization and control of fractional order chaotic systems. Nonlinear Dyn. **89**(3), 2065–2083 (2017). https://doi.org/10.1007/s11071-017-3570-6

44. O. Eray, S. Tokat, The design of a fractional-order sliding mode controller with a time-varying sliding surface. Trans. Inst. Meas. Control **42**(16), 3196–3215 (2020). https://doi.org/10.1177/0142331220944626

45. P. Gao, G. Zhang, H. Ouyang, L. Mei, A sliding mode control with nonlinear fractional order PID sliding surface for the speed operation of surface-mounted PMSM drives based on an extended state observer. Math. Probl. Eng. **2019**, 1–13 (2019). https://doi.org/10.1155/2019/7130232

46. Y. Luo, Y. Chen, Y. Pi, Experimental study of fractional order proportional derivative controller synthesis for fractional order systems. Mechatronics **21**(1), 204–214 (2011). https://doi.org/10.1016/j.mechatronics.2010.10.004

47. C. Yin, Y. Chen, S.-M. Zhong, Fractional-order power rate type reaching law for sliding mode control of uncertain nonlinear system. IFAC-PapersOnLine **47**(3), 5369–5374 (2014). https://doi.org/10.3182/20140824-6-ZA-1003.01115

48. K. Rajagopal, S. Vaidyanathan, A. Karthikeyan, P. Duraisamy, Dynamic analysis and chaos suppression in a fractional order brushless DC motor. Electr. Eng. **99**(2), 721–733 (2017). https://doi.org/10.1007/s00202-016-0444-8

49. A.M.D. Almeida, M.K. Lenzi, E.K. Lenzi, A survey of fractional order calculus applications of multiple-input, multiple-output (MIMO) process control. Fractal Fract. **4**(2), 22 (2020). https://doi.org/10.3390/fractalfract4020022

50. Y. Chen, Applied fractional calculus in controls, in *2009 American Control Conference*, pp. 34–35 (2009). https://doi.org/10.1109/ACC.2009.5159794

51. P.R. Sahu, P.K. Hota, S. Panda, Power system stability enhancement by fractional order multi input SSSC based controller employing whale optimization algorithm. J. Electr. Syst. Inf. Technol. **5**(3), 326–336 (2018). https://doi.org/10.1016/j.jesit.2018.02.008

52. Z. Yang, Y. Wei, H. Zhang, P. Zhu, J. Wang, Fractional calculus and its application in capacitance modeling of power converter, in *2020 IEEE Sustainable Power and Energy Conference (iSPEC)*, pp. 31–35. IEEE, Chengdu, China (2020). https://doi.org/10.1109/iSPEC50848.2020.9351018. https://ieeexplore.ieee.org/document/9351018/. Accessed 22 June 2023

53. I. Pan, S. Das, Fractional order AGC for distributed energy resources using robust optimization. IEEE Trans. Smart Grid **7**(5), 2175–2186 (2016). https://doi.org/10.1109/TSG.2015.2459766

54. N. Kuznetsov, Hidden attractors in fundamental problems and engineering models: a short survey, vol. 371, pp. 13–25 (2016). https://doi.org/10.1007/978-3-319-27247-4_2

55. B. Munmuangsaen, B. Srisuchinwong, A hidden chaotic attractor in the classical Lorenz system. Chaos Solitons Fractals **107**, 61–66 (2018). https://doi.org/10.1016/j.chaos.2017.12.017

56. Q. Yuan, F.-Y. Yang, L. Wang, A note on hidden transient chaos in the Lorenz system. Int. J. Nonlinear Sci. Numer. Simul. **18**(5), 427–434 (2017). https://doi.org/10.1515/ijnsns-2016-0168

57. G.-Q. Xia, S.-C. Chan, J. Liu, Multistability in a semiconductor laser with optoelectronic feedback. Opt. Express **15**, 572–6 (2007). https://doi.org/10.1364/OE.15.000572

58. R. Meucci, J.M. Ginoux, M. Mehrabbeik, S. Jafari, J.C. Sprott, Generalized multistability and its control in a laser. Chaos Interdiscip. J. Nonlinear Sci. **32**, 083111 (2022). https://doi.org/10.1063/5.0093727

59. M.A. Kiseleva, N.V. Kuznetsov, G.A. Leonov, P. Neittaanmäki, Hidden oscillations in drilling system actuated by induction motor. IFAC-PapersOnLine **46**(12), 86–89 (2013)

60. P. Faradja, G. Qi, Analysis of multistability, hidden chaos and transient chaos in brushless DC motor. Chaos Solitons Fractals **132**, 109606 (2020)

61. J.P. Singh, B.K. Roy, N.V. Kuznetsov, Multistability and hidden attractors in the dynamics of permanent magnet synchronous motor. Int. J. Bifurc. Chaos **29**(04), 1950056 (2019). https://doi.org/10.1142/S0218127419500561

62. Z.T. Zhusubaliyev, E. Mosekilde, V.G. Rubanov, R.A. Nabokov, Multistability and hidden attractors in a relay system with hysteresis. Phys. D Nonlinear Phenom. **306**, 6–15 (2015). https://doi.org/10.1016/j.physd.2015.05.005

63. S. Kelso, Multistability and metastability: understanding dynamic coordination in the brain. Philos. Trans. R. Soc. Lond. Ser. B Biol. Sci. **367**, 906–18 (2012). https://doi.org/10.1098/rstb.2011.0351

64. C. Manchein, L. Santana, R.M. da Silva, M.W. Beims, Noise-induced stabilization of the Fitzhugh-Nagumo neuron dynamics: multistability and transient chaos.

2436

Eur. Phys. J. Spec. Top. (2023) 232:2415–2436

Chaos Interdiscip. J. Nonlinear Sci. **32**, 083102 (2022). https://doi.org/10.1063/5.0086994

65. S. Fang, S. Zhou, D. Yurchenko, T. Yang, W.-H. Liao, Multistability phenomenon in signal processing, energy harvesting, composite structures, and metamaterials: a review. Mech. Syst. Signal Process. **166**, 108419 (2022). https://doi.org/10.1016/j.ymssp.2021.108419

66. S. Jafari, J.C. Sprott, F. Nazarimehr, Recent new examples of hidden attractors. Eur. Phys. J. Spec. Top. **224**(8), 1469–1476 (2015). https://doi.org/10.1140/epjst/e2015-02472-1

67. B. Zhang, Y. Pi, Y. Luo, Fractional order sliding-mode control based on parameters auto-tuning for velocity control of permanent magnet synchronous motor. ISA Trans. **51**(5), 649–656 (2012). https://doi.org/10.1016/j.isatra.2012.04.006

68. A. Dumlu, Design of a fractional-order adaptive integral sliding mode controller for the trajectory tracking control of robot manipulators. Proc. Inst. Mech. Eng. Part I J. Syst. Control Eng. **232**, 095965181877821 (2018). https://doi.org/10.1177/0959651818778218

69. T. Zhou, Y.-G. Xu, B. Wu, Smooth fractional order sliding mode controller for spherical robots with input saturation. Appl. Sci. **10**(6), 2117 (2020). https://doi.org/10.3390/app10062117

70. G. Zhong, H. Deng, J. Li, Retraction note to: chattering-free variable structure controller design via fractional calculus approach and its application. Nonlinear Dyn. **100**(1), 541 (2020). https://doi.org/10.1007/s11071-020-05513-w

71. J. Arunshankar, Control of nonlinear two-tank hybrid system using sliding mode controller with fractional-order PI-D sliding surface. Comput. Electr. Eng. **71**, 953–965 (2018). https://doi.org/10.1016/j.compeleceng.2017.10.005

72. S. Razmara, M. Yahyazadeh, H.F. Marj, Novel flexible sliding mode control for projective synchronization of mismatched time-delayed fractional-order nonlinear systems with unknown parameters and disturbances. Iran. J. Sci. Technol. Trans. Electr. Eng. **45**(2), 553–571 (2021). https://doi.org/10.1007/s40998-020-00386-6

73. S. Sheykhi, H. Gholizade Narm, Providing robust-adaptive fractional-order sliding mode control in hybrid adaptive cruise control systems in the presence of model uncertainties and external disturbances. Int. J. Dyn. Control **10**, 1–13 (2022). https://doi.org/10.1007/s40435-022-00936-2

74. I. Podlubny, Fractional Differential Equations: An Introduction to Fractional Derivatives, Fractional Differential Equations, to Methods of Their Solution and Some of Their Applications. Mathematics in Science and Engineering, vol. 198. Academic Press, San Diego (1999)

75. A. Wolf, J. Swift, H. Swinney, J. Vastano, Determining Lyapunov exponents from a time series. Phys. D Nonlinear Phenom. **16**, 285–317 (1985). https://doi.org/10.1016/0167-2789(85)90011-9

76. N. Aguila-Camacho, M.A. Duarte-Mermoud, J.A. Gallegos, Lyapunov functions for fractional order systems. Commun. Nonlinear Sci. Numer. Simul. **19**(9), 2951–2957 (2014). https://doi.org/10.1016/j.cnsns.2014.01.022

77. M.S. Tavazoei, M. Haeri, A necessary condition for double scroll attractor existence in fractional-order systems. Phys. Lett. A **367**(1–2), 102–113 (2007). https://doi.org/10.1016/j.physleta.2007.05.081

78. V. Venkatasubramanian, W. Ji, Coexistence of four different attractors in a fundamental power system model. IEEE Trans. Circuits Syst. I Fundam. Theory Appl. **46**(3), 405–409 (1999). https://doi.org/10.1109/81.751316